AN ABSTRACT OF THE THESIS OF

STEPHEN LYNN POOLE for the MASTER OF SCIENCE
(Name) (Degree)

in Oceanography presented on June 24, 1974
(Major Department) (Date)

Title: THE EFFECT OF THE LAND BREEZE ON THE MESOSCALE WIND FIELD OFF THE OREGON COAST

Abstract approved: Redacted for privacy
Wayne V. Burt

Two land breeze events occurred off the Oregon coast on the nights of April 19th and 20th, 1973. An array of four moored toroid buoys and one land station recorded the effect of the land breeze event on the surface mesoscale wind and temperature fields. The land breezes may have resulted from the premature summerly conditions of fair weather and southward coastal winds that were caused by an early northeastward extension of the North Pacific High.

The main features of the events were as follows:

1) A cooling period of a few hours after sunset established an air temperature gradient of -0.1° C km^{-1} in the nearshore 10 km region.

2) The advance of the land breeze front produced a 5° C temperature drop at the land station and a 1° C temperature drop at the buoy stations.

3) Simultaneously, the front also caused a decrease in wind speed by about an order of magnitude at each of the stations. During the passage of the front the wind veered from southward at 10 m sec^{-1} to westward at 2 to 3 m sec^{-1}.

4) At dawn the temperature gradient was rapidly reversed, but there was a 2 hour lag before the wind speed began to increase. No frontal return flow was observed, instead the wind backed to the south and increased gradually over the array.

Horizontal divergence and vertical vorticity were calculated using a simplified program. The land breeze produced spans of positive vorticity ($5 \times 10^{-4} sec^{-1}$) over the array, possibly due to the horizontal wind shear in the offshore direction. The land breeze also caused a zone of convergence over the nearshore 10 km. The convergence was preceeded by a brief period of intense divergence.

There was no convergence zone beyond the nearshore region. Instead there appeared alternating bands of convergence and divergence with a period of around 37 minutes. The same periodicity was observed in the offshore wind velocity. These features can be explained by a model of horizontal roll vortices migrating seaward from the nearshore convergence zone. The roll wavelength is inferred to be 4.7 km, the westward migration speed is 2 m sec^{-1}, and the height of the PBL is estimated to be 1.5 km. This leads to a

PBL Reynolds number of 370 $\pm$ 80, which is lower than previous observations and suggests that the rolls are produced by buoyancy and parallel instability. A model which is compatible with all the above is presented.

The Effect of the Land Breeze on the Mesoscale Wind Field off the Oregon Coast

by

Stephen Lynn Poole

A THESIS

submitted to

Oregon State University

in partial fulfillment of
the requirements for the
degree of

Master of Science

June 1975

APPROVED:

Redacted for privacy

Professor of Oceanography
in charge of major

Redacted for privacy

Dean of School of Oceanography

Redacted for privacy

Dean of Graduate School

Date thesis is presented June 24, 1974

Typed by Susie Kozlik for Stephen Lynn Poole

ACKNOWLEDGEMENTS

I wish to give special thanks to Dr. Wayne V. Burt, whose supervision, advice and support made this thesis possible.

Thanks are also due to Dr. Henry Crew and Dr. Larry Mahrt for their assistance in analyzing the data and their many suggestions which helped to improve this thesis.

I wish also to thank Dr. William Quinn for his advice on meteorological aspects of the research. To Asa Robinson and Robert Hansen, for their assistance in the collection and analysis of this data, I also give many thanks.

This research was supported by the Global Atmospheric Research program of the National Science Foundation under Grant GA 28004.

TABLE OF CONTENTS

Section		Page
I	INTRODUCTION	1
II	DATA COLLECTION AND REDUCTION	6
	Observational Program	6
	Synoptic Situation	9
III	PRIMARY FEATURES OF THE LAND BREEZE EVENTS	13
	Station Data	13
	Divergence and Vorticity	30
IV	HORIZONTAL ROLL VORTICES	44
V	CONCLUSIONS	71
	BIBLIOGRAPHY	75
	APPENDIX: Program DIVORT	78

LIST OF FIGURES

Figure		Page
1	Observational Array	7
2	Surface Synoptic Situation at 1800Z, 20 April 1973	11
3	Station 1 Time Series	14
4	Station 2 Time Series	15
5	Station 3 Time Series	16
6	Station 4 Time Series	17
7	Station 5 Time Series	18
8	Hourly Winds and Temperature over the Array	
	a. Event I	20
	b. Event II	21
9	Progressive Vector Diagrams For All Stations	28
10	Hypothetical Buoy Array for Computation of Divergence and Vorticity Using DIVORT	32
11	Divergence and Vorticity in Triangle A	36
12	Divergence and Vorticity in Triangle B	37
13	Divergence and Vorticity in Triangle C	38
14	Schematic of Horizontal Roll Vortices	45
15	Spectral Analysis of Divergence During Event I	49
16	Spectral Analysis of Divergence During Event II	50
17	Analysis of Station 5 U-Component	
	a. Event I	52
	b. Event II	53
18	Analysis of Station 4 U-Component	
	a. Event I	54
	b. Event II	55

Figure		Page
19	Analysis of Station 3 U-Component	
	a. Event I	56
	b. Event II	57
20	Models of Roll Dimensions	61
21	Hypothetical Situation Showing Land Breeze and Horizontal Roll Vortices	69

THE EFFECT OF THE LAND BREEZE ON THE MESOSCALE WIND FIELD OFF THE OREGON COAST

INTRODUCTION

Over the years the sea breeze has received attention as a significant interaction between the ocean and the atmosphere. The same thermodynamic processes that drive the sea breeze are also responsible for an important, but much less studied phenomenon--the land breeze. During an investigation of the mesoscale wind field off the Oregon coast in April, 1973, two land breeze events were recorded, revealing a wealth of information on the structure of the land breeze and its effect on the coastal wind field. This thesis will examine the two land breezes, describing their general features and peculiarities, and will attempt to explain unusual phenomena that occurred during the events.

We begin with a review of the dynamics responsible for both the sea breeze and land breeze, the products of an interesting interaction between sun, land, sea and air. Differential heating supplies the energy for this coastal air circulation. Imagine a body of air at rest over a coastline, so that it covers both land and ocean. During periods of fair weather solar radiation is absorbed by both the land and the sea, increasing their temperature. However, due to the high specific heat of water, the water temperature increases more slowly

than the land temperature. The air temperature over land will thus be higher than the air temperature over water, and a temperature gradient will exist from the land to the sea. This temperature gradient will manifest itself on the associated (by the equation of state for air) pressure and density fields. For a uniform sea level pressure, the pressure gradient will slope downwards towards the sea and the density gradient will slope downwards towards the land (so that as you move seaward you will encounter denser, i.e., colder, air).

The intersection of pressure and density gradients is called a pressure-density solenoid. The solenoid will try to adjust itself by driving the dense sea air beneath the less dense land air. This corresponds to our familiar picture of "the warm land air rises and is replaced by the cold air from the sea." The cold air replacement is the sea breeze, its intensity will depend on the magnitude of the land-sea temperature gradient and surface friction (Haurwitz, 1947).

Numerous observational and theoretical studies have been made of the sea breeze. In addition to Haurwitz, models have been proposed by Estoque (1961, 1962) and Hsu (1970). Sea breezes off Texas have been investigated by Hsu (1970) and Eddy (1966), off New England by Fisher (1960), and recently off Oregon by O'Brien and Johnson (1973). These various studies report upper level return flow of the land air, wind speeds in excess of 20 knots and inland penetrations of over 80 km, which has a strong influence on local weather.

By contrast the land breeze is less vigorous than the sea breeze. It is produced by weak gradients, blowing seaward, affecting only nearshore regions. It is usually ignored in studies of the sea breeze. Whereas the sea breeze is a product of daytime heating, the land breeze results from nighttime cooling. After sunset both land and sea experience a net decrease in temperature, but due to its high specific heat, the sea temperature changes more slowly than the land temperature. The land cooling will be comparitively rapid, especially on clear nights when intense radiational cooling takes place at the land surface. The land air eventually becomes cooler than the sea air and a reverse temperature gradient is established. However, this temperature gradient may be an order of magnitude less than the daytime gradient, so the resulting circulation is much less intense than for the sea breeze. Unless the sea temperature is unusually warm, as in the tropics, the land breeze will be only a few knots and will not extend more than 20 km from the coast. On the Oregon coast the cold ocean temperature makes for strong sea breezes, but extremely weak land breezes, if any at all.

Observations of land breeze are confined to passing references during observations of sea breeze. Presumably seldom, if ever, is the land breeze studied by itself (the author could not locate any such study). This is understandable due to the weakness and the offshore location of the events--oceanic weather stations are few and far

between. Generally the only offshore data on winds comes from ships (Fisher), offshore oil rigs (Hsu), and assorted buoys (O'Brien and Johnson used data from CUEA buoys). The resulting picture of the land breeze has been incomplete and sketchy at best.

However, by using automated, self-recording meteorological buoys, placed in an appropriate grid, the offshore land breeze and other mesoscale phenomena can be studied in great detail. The results of such a study should show that the land breeze is not merely a weakened sea breeze blowing the other way, but it should exhibit some unique properties. For example, the structure of the land breeze should be radically affected by the ocean, with its high specific heat and low skin friction. Also, whereas the sea breeze is a strong wind blowing into a relatively calm land air mass, the land breeze is low velocity land air trying to force its way into the usually strong (off Oregon, at least) oceanic wind field. The results should be complex and interesting.

Such a study was made in April, 1973, on the Oregon coast. Data were collected from one land station and four buoys that were located offshore in a study of the mesoscale wind field near the shore line. During the period of observation two interesting land breeze events occurred on consecutive nights and were recorded. Section II of this thesis will detail the equipment used in this study, its location, and the unusual synoptic situation which produced the land breezes.

Section III will deal with the station data and will demonstrate the striking effect that the land breeze had on the coastal wind field. Also in Section III are plots of the divergence and vorticity over the array, which reveal intense convergence in the nearshore region, positive vorticity, and intriguing periodicities in the wind field farther offshore during the events. Section IV will further examine the offshore periodicities of divergence and wind speed and will attempt to explain them as evidence of horizontal roll vortices generated by the land breeze convergence. The author hopes to show that, far from being a minor side effect, the land breeze is a fascinating collection of mesoscale interactions and is worthy of much further investigation.

II. DATA COLLECTION AND REDUCTION

Observational Program

The observational network consisted of one land station and four moored toroid buoys. Each station was equipped with data recorders and sensors to measure wind speed and wind direction. The data loggers, wind speed, and wind direction and compass instruments were manufactured by Ivar Aanderaa of Bergen, Norway. All stations recorded air temperature and the moored buoys also recorded sea temperature. All instruments were calibrated before the cruise and recalibrated after the cruise.

The land station, Station 1, was erected at Ona Beach State Park, at the mouth of Beaver Creek (44° 31' N, 124° 5' W), which is about 10 miles south of Newport, Oregon. The buoys were moored in an array perpendicular to the coast at the location of the land station. The array formed three roughly equilateral triangles of six to seven kilometers to a side. The farthest buoy, Station 5, was 14.2 km offshore. (See Figure 1).

Running north-south, this section of the Oregon coastline rises into eroded, sandy bluffs about 100 feet high. The bluffs are cut by various streams--such as Beaver Creek, which forms a shallow valley opening towards the northwest (305° T). Offshore the continental shelf slopes gently down to the west so that the depth at Station 5

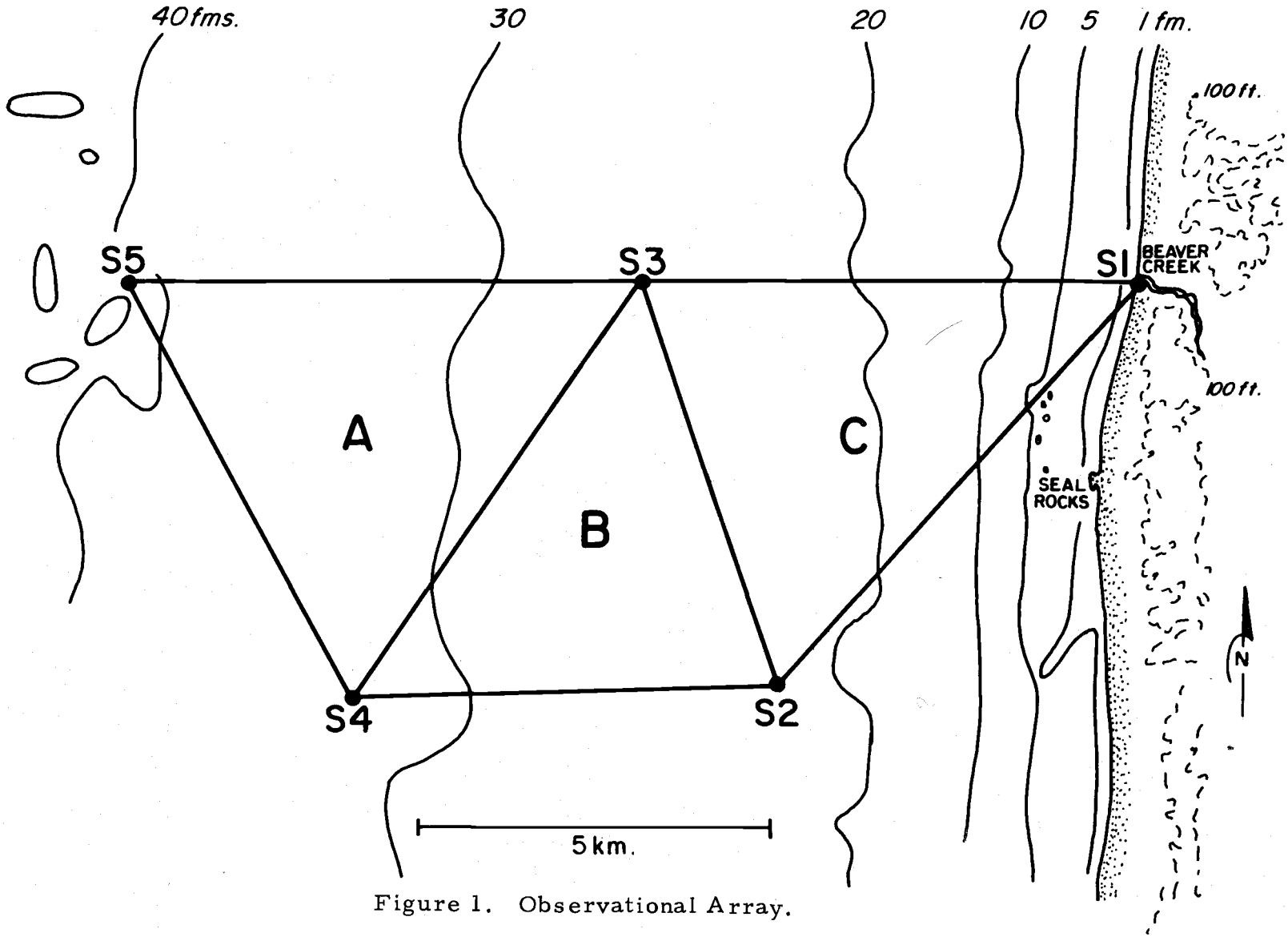

Figure 1. Observational Array.

is only 40 fathoms. South of Ona Beach are some impressive igneous outcroppings--Seal Rocks--but in general there are no major topographic features to impede a north-south current or a seaward breeze.

The data loggers were set to record at a sampling rate of 1.25 minutes. Wind speed was integrated during the sampling interval by counting the revolution of a cup anemometer. The other observations were instantaneous. Simultaneous good data were collected from all stations from 1330 PST on April 19 until 1120 PST on April 21 (Pacific Standard Time is used throughout this paper). Thus 45 hours of data were collected, covering two nights and two land breeze events. At this time of year sunrise was at 0522 and sunset was at 1905.

The data loggers stored data in digital form on magnetic tape. The data were converted from digital to physical form on Oregon State University's CDC 3300. All data analysis was also accomplished on the CDC 3300. The 1.25 minute data were smoothed by taking 10 minute averages, and for a very general picture of the events hourly averages were also computed. Divergence and vorticity were computed from the 10 minute averaged data and plotted along with all time series and progressive vector diagrams (PVD's) on the CDC 3300's Calcomp plotter. (For more information on data storage and reduction, see Cummings, 1973).

Synoptic Situation

The winds off Oregon are normally related to two oceanic pressure centers, the North Pacific High and the Aleutian Low. The wind fields fall into two distinct modes--winter and summer--depending on the location of the pressure centers. During the summer, the North Pacific High achieves its greatest development of about 1025 mb and is centered at 30 - 40° N and 150° W. The Aleutian Low is weak at this time. The geostrophic wind coming around the high approaches the Pacific Northwest Coast from the north or northwest. The Coastal Range deflects the surface winds so that they tend to follow the coastline. In winter months the North Pacific High moves about 10° southward while the Aleutian Low deepens. The flow around the low reaches the Oregon coast from the southwest, sometimes with gale force.

Spring and fall are periods of variable winds and generally fair weather. The situation during April is between the winter and summer modes, but more strongly influenced by the winter conditions. The average offshore winds during April, as determined from the geostrophic wind field from 1961 to 1963, were mainly from the WSW with a mean speed of about 8 knots (Bourke, et al., 1971).

It is therefore surprising that the predominant wind recorded during April 19 through 21, 1973 was from the north at about 5 knots--a situation usually not found until June or July.

These apparent summertime conditions appeared in April due to an unusual, premature shift of the North Pacific High. The week of April 15 through 22 began with the typical cold fronts moving onto the Oregon coast from the North Pacific. Surface coastal winds on Tuesday, April 19, were from the southwest at 10 knots, the expected April condition. At this time the Aleutian Low was at 990 mb and just south of Kodiak Island. The North Pacific High was up to 1032 mb and spread out between 35 - 40° N and 140 - 145° W. On Wednesday the High began intensifying, reaching 1037 mb, and extending towards the northeast, filling in behind the last cold frontal passage. Another cold front developed on Wednesday, its low pressure center moving over Vancouver Island, and tended to push the High pressure intrusion back south. Instead the front became occluded and tenuous and began to break up on Thursday. The North Pacific High quickly reintensified and pushed through the weak front. By Friday, April 20, a tongue of high pressure was west of Vancouver Island at 1033 mb. At 1000 hours Friday, halfway through the period of observation, the high center had reached 1038 mb and had elongated towards the northeast. Its location was now 40° N and 135° W, at least as far north as its normal summer location. (See Figure 2). The Aleutian Low was now farther south and west of Kodiak, at 996 mb. Oregon coastal winds came out of the north at 30 knots, and clear skies prevailed along the entire coast. Conditions remained this way

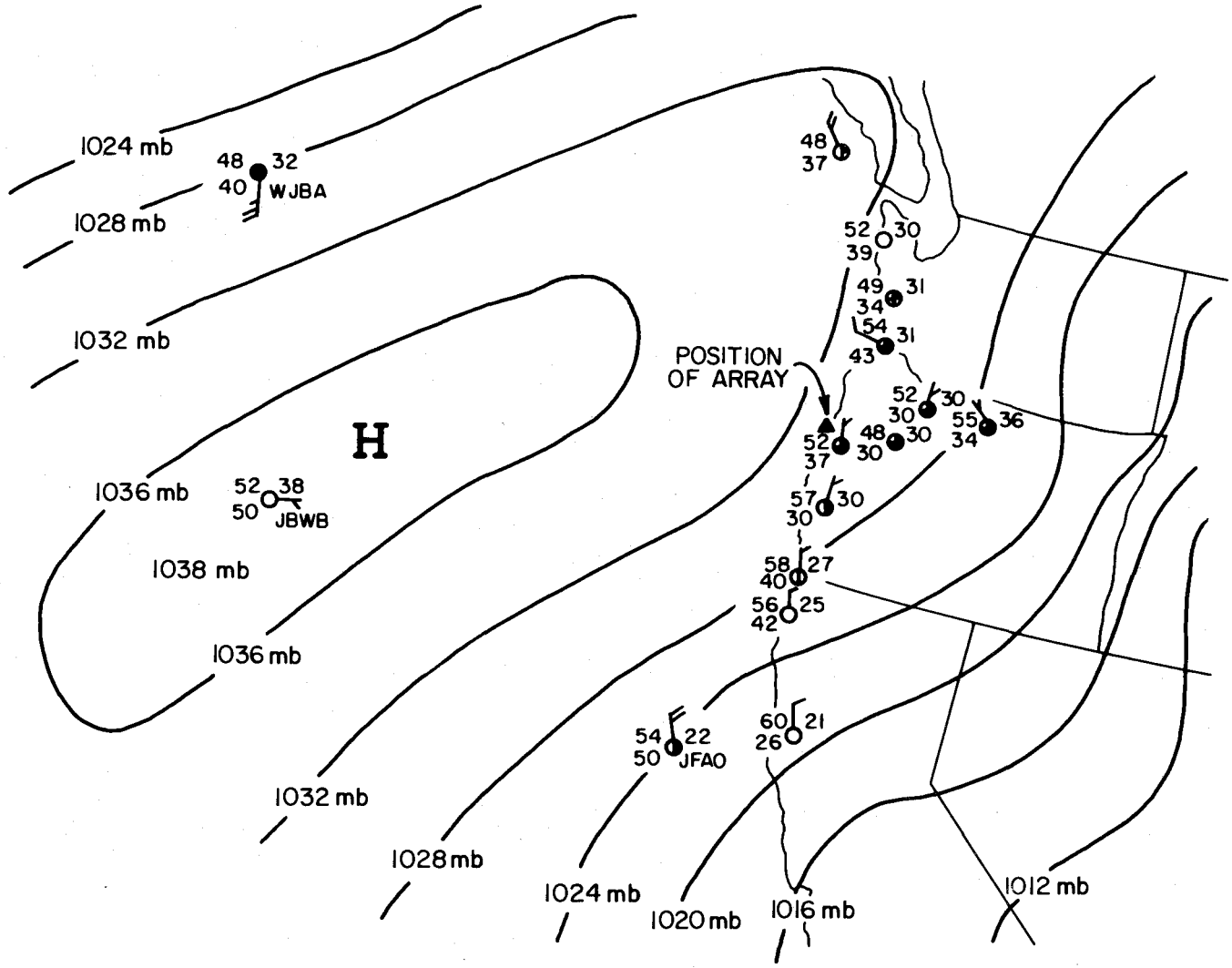

Figure 2. Surface Synoptic Situation at 1800Z, 20 April 1973.

throughout Friday and Saturday, and indeed the rest of April enjoyed more summerly weather due to the intense high pressure extension. By the end of April the high had moved back south and the pressure was down to 1024 mb.

It is difficult to determine the effect of this high pressure movement on the existence of the two land breeze events. It is possible that the land breezes were freak occurrences that resulted from summertime weather being imposed on springtime land and sea temperatures. Although the land station was in operation for five days, from April 17 until 21, the only evidence of land breezes was on the nights of the 19th and 20th. No sea breezes were observed during the entire period. The fair weather which accompanied the high permitted solar radiation to heat both land and sea, but possibly the mean land temperature was too cold to allow a pocket of warm land air to form which would have resulted in a sea breeze. Instead the clear, cold nights enhanced radiation cooling, creating a mass of land air colder than the adjacent sea air. The sea temperatures were not much affected by the extra radiation or cooling--their mean value for April is about 10° C, the temperature which was observed during the experiment. It is unfortunate that so few studies have been made of land breezes, especially off Oregon; they may be typical features of the spring weather conditions, or they could indeed be rare phenomena.

III. PRIMARY FEATURES OF THE LAND BREEZE EVENTS

Station Data

The two land breeze events which occurred during the period of observation will hereafter be referred to as Event I (April 19 to 20) and Event II (April 20 to 21). Also for convenience the land station and the four buoy stations will be abbreviated as S1, S2, S3, S4 and S5 respectively (Figure 1).

Figures 3 through 7 show the time series plots of the 10 minute averaged data from each station. Presented are wind speed, u-component of wind velocity (positive to the east), v-component of velocity (positive to the north), and a combination plot of air and sea temperatures. The wind speed plot is labeled with "Event I" and "Event II" to identify the general sections affected by the events.

The north-south orientation of the Oregon coast fits neatly into an $\underline{x}$ (east-west) and $\underline{y}$ (north-south) terrestrial coordinate system. Thus an offshore breeze such as a land breeze will appear as a negative u velocity component. A southward wind will be negative v velocity component. Because of the high pressure center due west of the Pacific Coast, we can expect winds to the south to be prevalent. The plots confirm this--the wind at S5, which is least affected by the land breeze, is mostly a strong negative v velocity flow, as much as

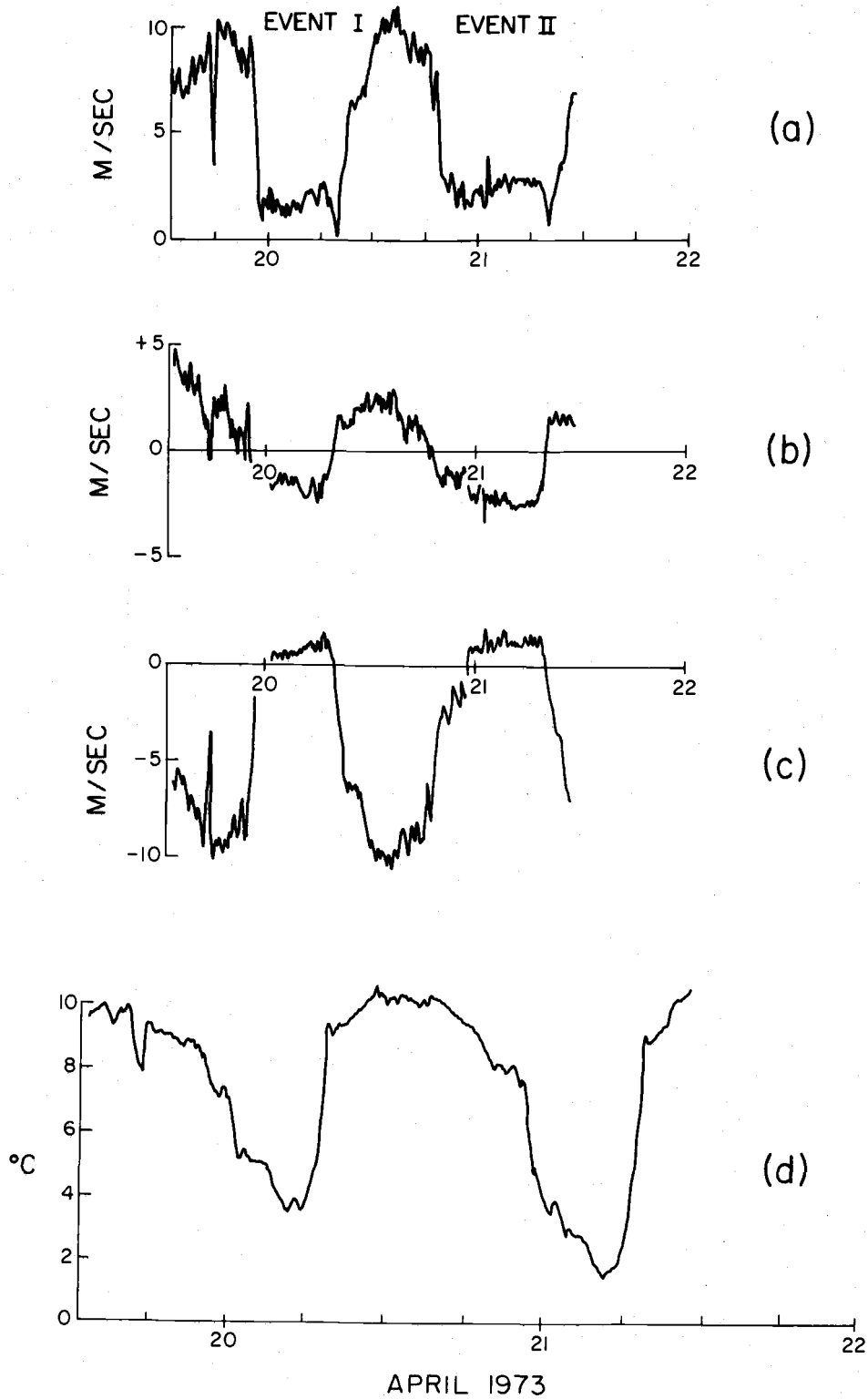

Figure 3. Station 1. (a) Wind Speed, (b) U-Component and (c) V-Component of Wind Velocity, (d) Air Temperature.

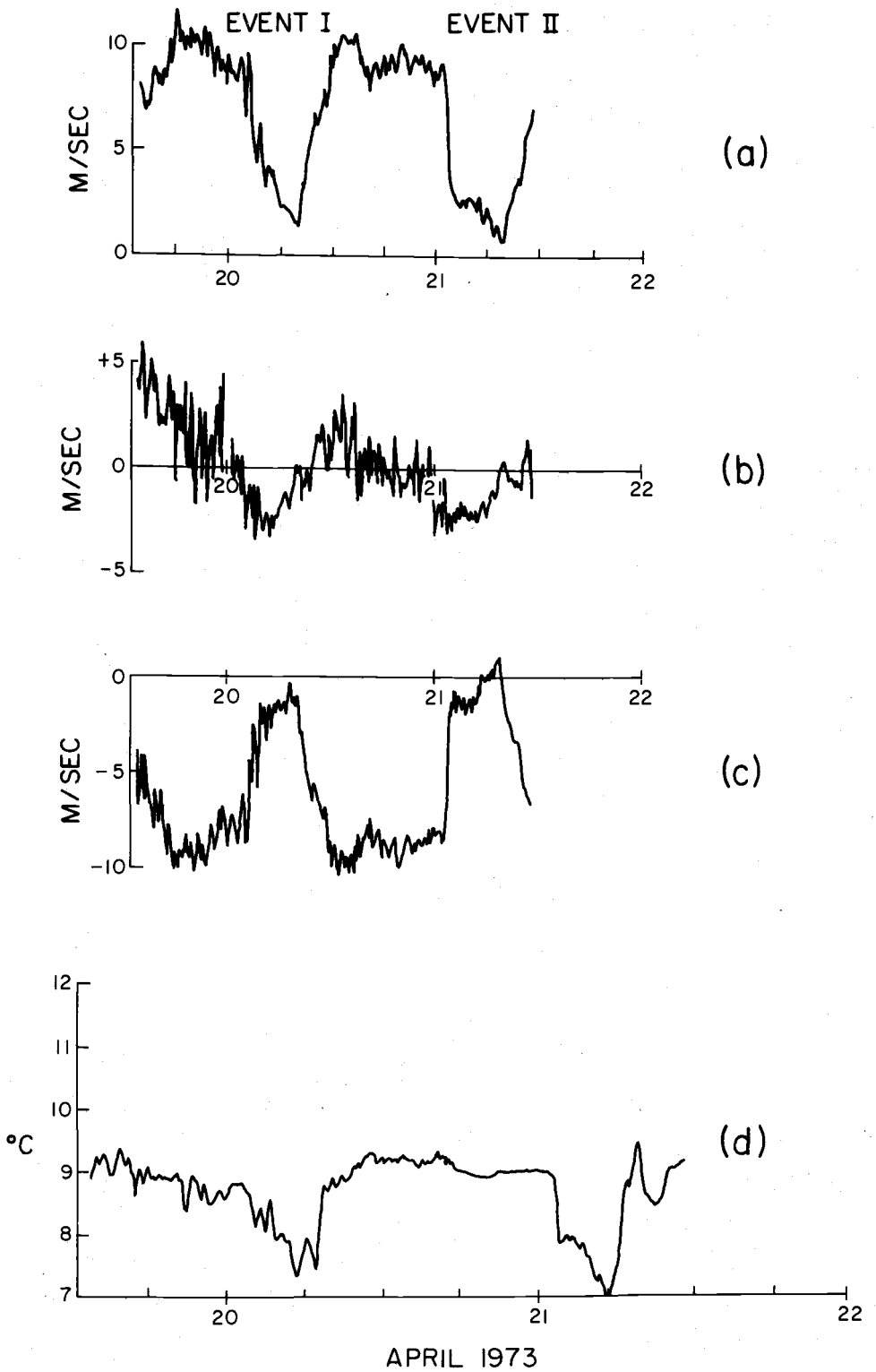

Figure 4. Station 2. (a) Wind Speed, (b) U-Component and (c) V-Component of Wind Velocity, (d) Air Temperature.

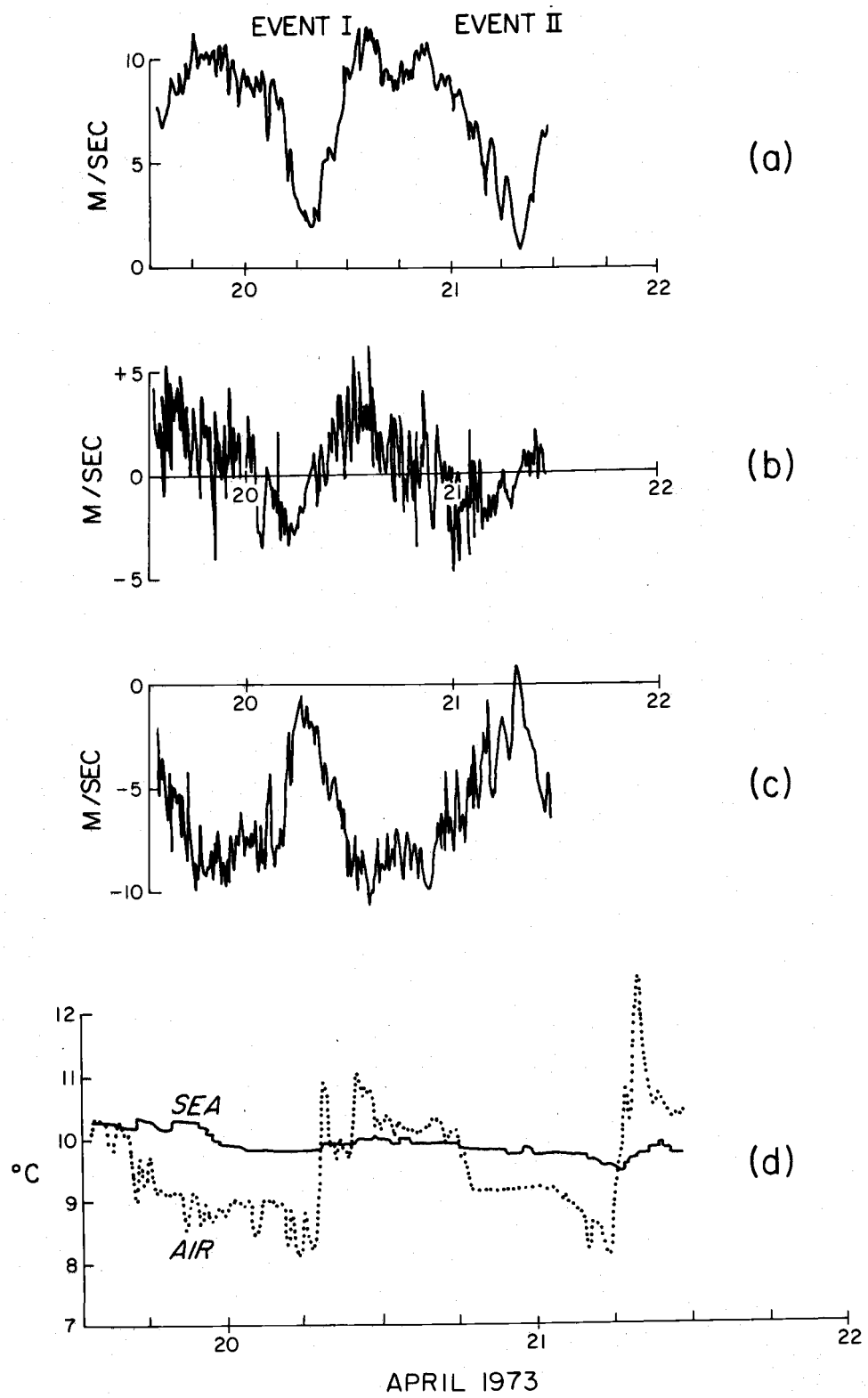

Figure 5. Station 3. (a) Wind Speed, (b) U-Component and (c) V-Component of Wind Velocity, (d) Air and Sea Temperature.

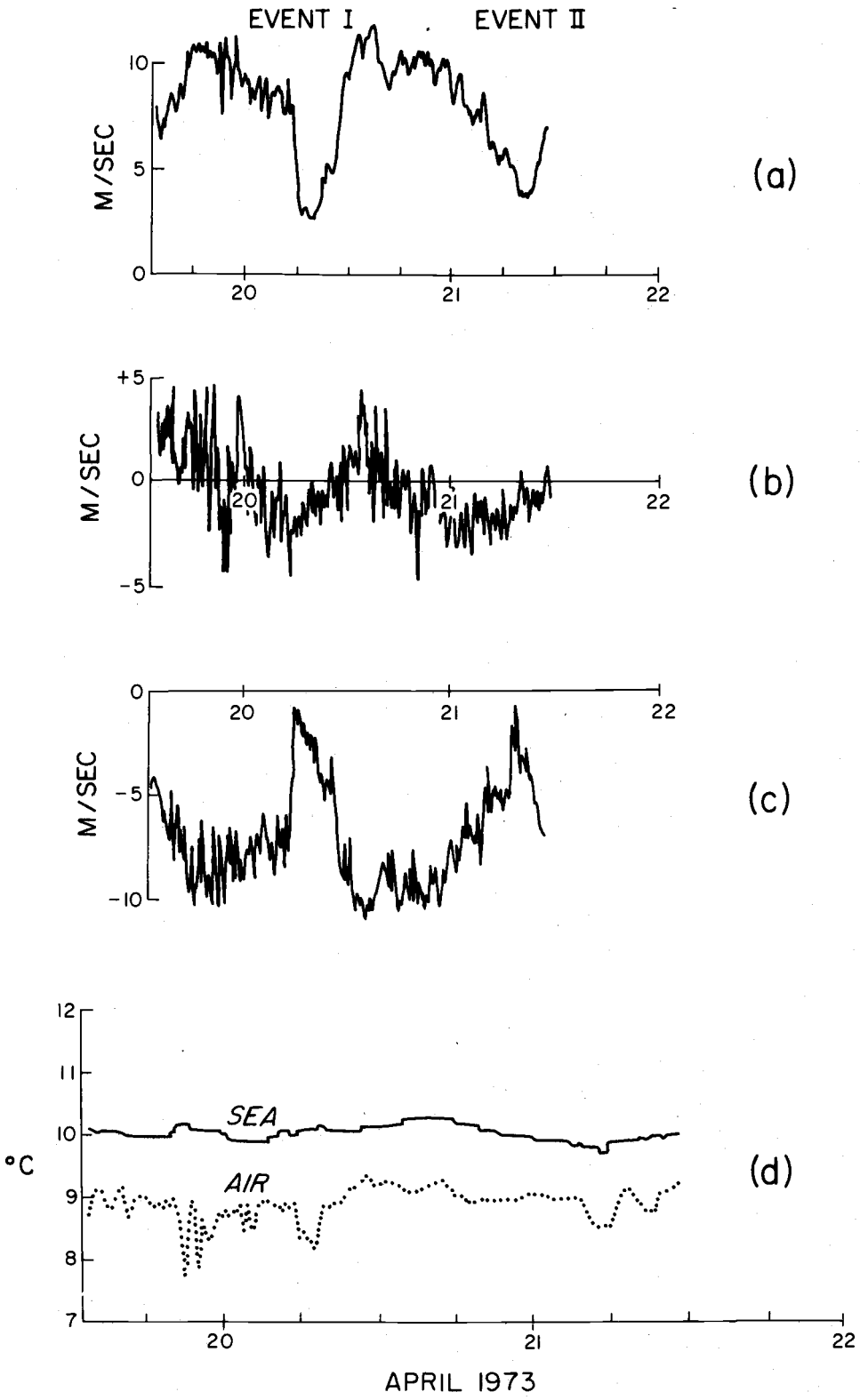

Figure 6. Station 4. (a) Wind Speed, (b) U-Component and (c) V-Component of Wind Velocity, (d) Air and Sea Temperature.

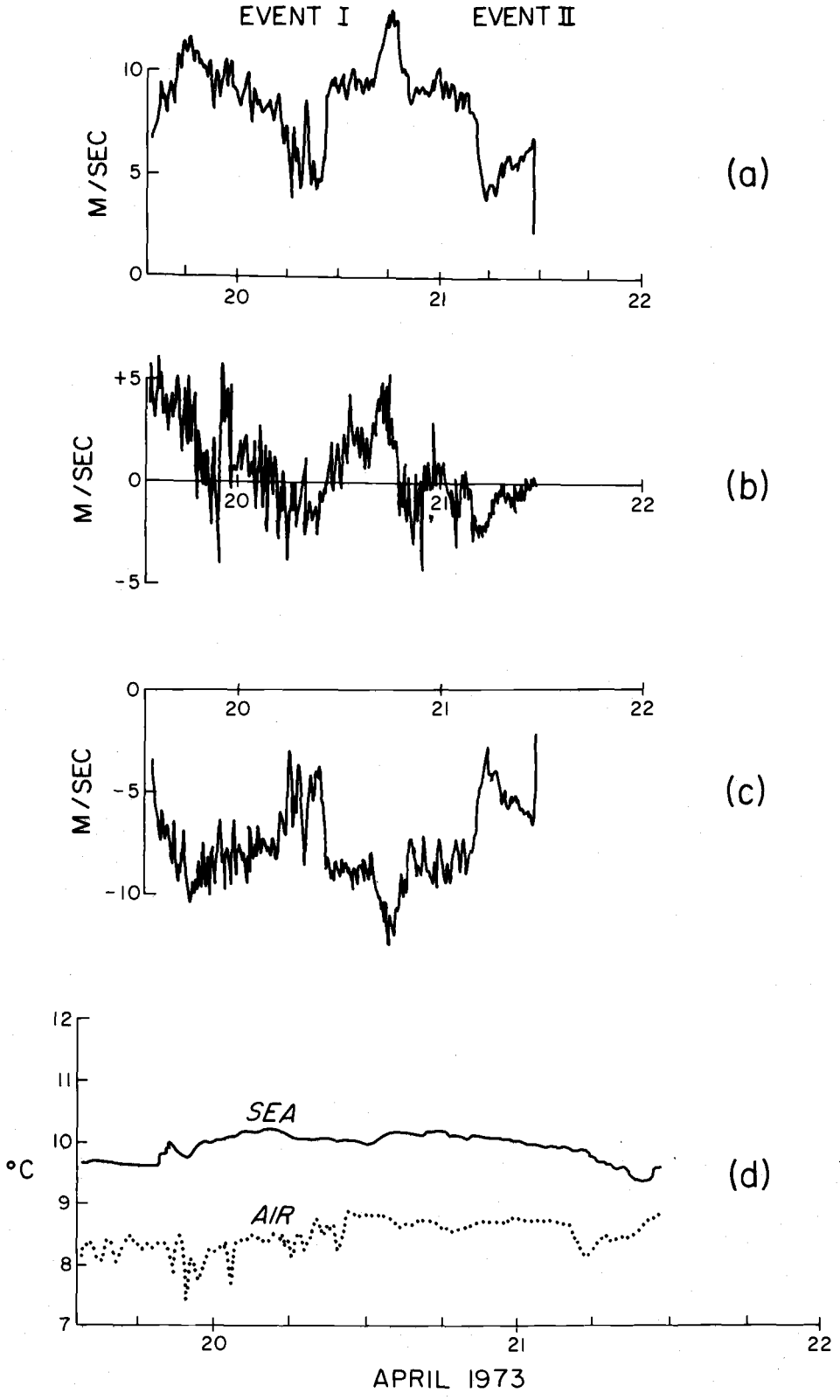

Figure 7. Station 5. (a) Wind Speed, (b) U-Component and (c) V-Component of Wind Velocity, (d) Air and Sea Temperature.

13 m/sec at one time. Having noted this we can proceed to see how the prevailing wind is affected by the weak, westward blowing land breeze.

First we shall examine the chronology of the general features of Event I and then continue to a comparison with Event II. Figure 8a portrays the history of the temperature gradient between the stations during Event I. It is drawn from hourly averages of temperature and thus presents only a rough picture of the actual gradient. We can see that the steepest gradients are between S1 and S2, where, just before dawn, the maximum gradient of 1° C/km occurs. By comparison the gradients between the buoy stations are almost negligible, the steepest being about 0.25° C/km. Here we can see how strongly air temperature is affected by the substance below--long after the land air has reached its minimum temperature, the sea air is still approximately at its daytime temperature, due to the constant upward transfer of heat from the ocean. We can postulate that the land breeze will be a nearshore phenomena, not extending much past S3, since the seaward gradients are much shallower.

The local rate of change of temperature during adiabatic flow is the sum of two terms, an advection term and the local cooling-heating term, $\underline{Q}$:

$$\frac{\partial T}{\partial t} = u\frac{\partial T}{\partial x} + Q.$$

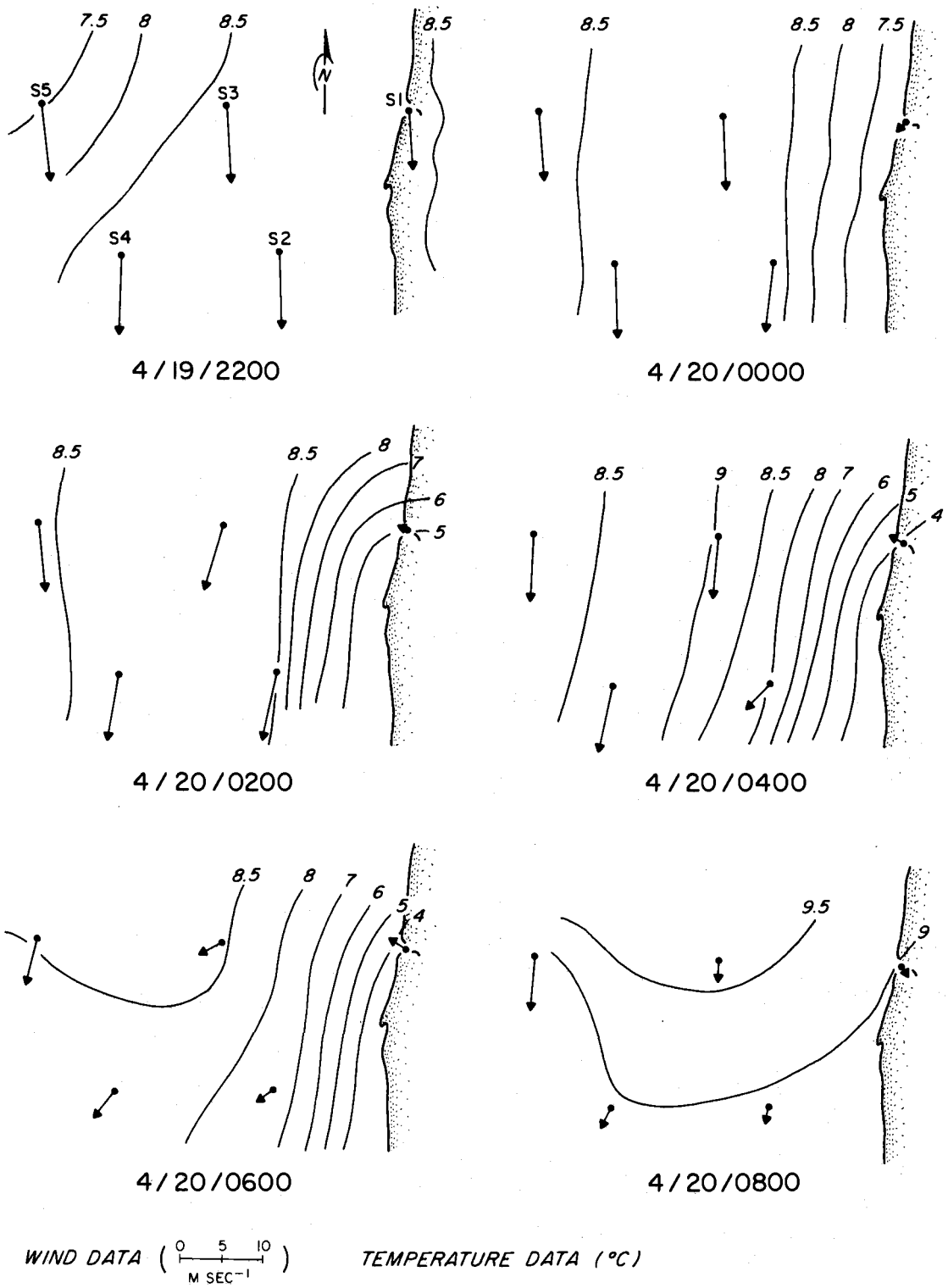

Figure 8a. Hourly Winds and Air Temperature, Event I.

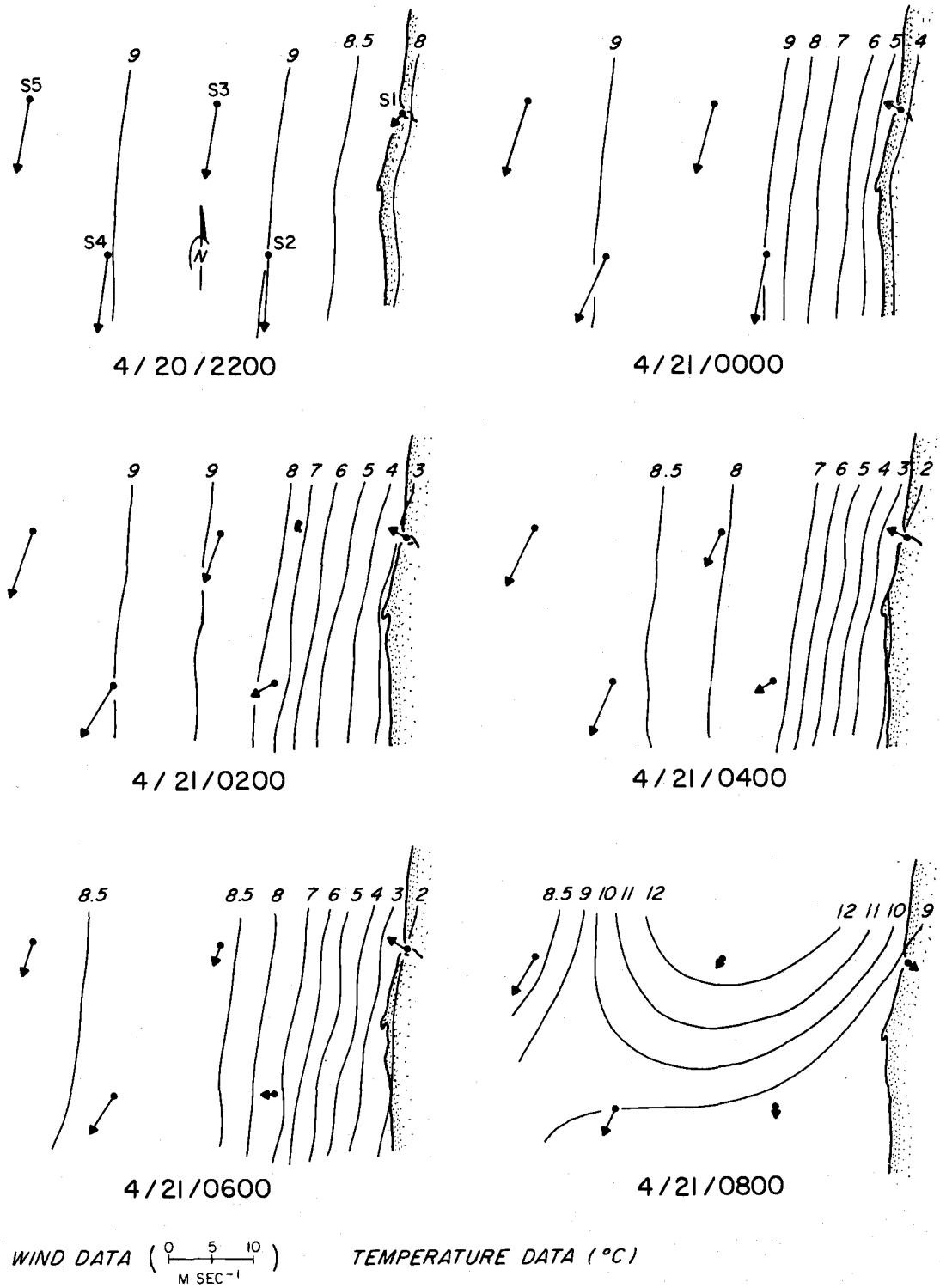

Figure 8b. Hourly Winds and Air Temperature, Event II.

Here we assume that the advection is due to the horizontal velocity field and that $\left| u \frac{\partial T}{\partial x} \right| >> \left| v \frac{\partial T}{\partial y} \right|$. The $\underline{Q}$ term corresponds to the cooling that occurs after sunset. The rate of decrease in air temperature at S4 and S5 is small due to the stabilizing effect of the warmer sea water.

The second temperature change is caused by the advection of cool land air by the land breeze. This drop occurs at S1 at 2300 and about seven hours later at S4 and S5. We can follow the land breeze front as it arrives at the different stations by noting a temperature drop and a corresponding decrease in wind speed. The two features arrive at S1 at 2300. The u-component becomes negative at this time and the v-component drops sharply and eventually becomes positive. (This positive v-component does not appear at the other stations. It can possibly be explained by noting that the wind direction at 0600 is 300° and remembering that Beaver Creek valley opens toward 305°. Thus the land breeze at this part of the coast may be funneled towards the northwest while the breeze on either side of Beaver Creek Valley is towards the west.)

It is possible to recognize these features--temperature drop and wind speed decrease--at the other stations and to compile a simple timetable for the event: leave S1 at 2300, arrive S2 at 0200, arrive S3 at 0400, and arrive almost simultaneously at S4 and S5 at 0500. Paradoxically, the front seems to progress slowly to the

nearshore S2 and S3 and then accelerate to S4 and S5. This is probably a consequence of the geometry of the buoy array: if the prevailing wind diverts the westward moving front until it is moving southwestward, then it will be traveling normal to the line connecting S4 and S5 and will arrive at both stations at the same time.

The front is not a steady, homogeneous phenomena. It arrives dramatically at S1, S2, and S4, but comes in bursts to S3 and S5. The extreme temperature drops at S1 seem to come in stages, as if progressively colder air from farther inland is arriving at the station, advected down by the land breeze. It is difficult to determine the exact arrival time of the front at the offshore stations. The times above are only approximate. The picture is confused by cold air moving southward with prevailing wind; two cold spurts are seen simultaneously at S3, S4 and S5 beginning around 2100. The wind at this time for these stations is still predominantly negative v, so presumably the cold air has been entrained farther up the coast and advected southward, and is not part of the local land breeze.

The major features of the event can be summarized as follows:

1) There is a steep nearshore temperature gradient which is established after sunset, with shallower gradients offshore.

2) The arrival of the land breeze front is denoted by a drop in temperature of about 5° C at the land station S1 and less than 1° C at the buoy stations.

3) Correspondingly, there is a decrease in wind speed by about an order of magnitude from the daytime value. There is less decrease farther offshore. Daytime wind speeds are about 10 m/sec. Wind speeds during the land breeze are 2 to 3 m/sec.

4) The wind velocity vector veers and becomes westward, as seen in the decreasing negative v-component accompanied by and increasing negative u-component. The v/u ratio during the daytime is about 10; during the land breeze this ratio falls to about 1.

5) After dawn there is a rapid reversal of all the above features.

Perhaps the feature that most distinguishes this land breeze from a sea breeze is that the wind speed <u>decreases</u> during the event, it does not increase as in a sea breeze. The difference lies in the fact that the land air mass is relatively calm while the sea air mass is flowing south under geostrophic influence. When the pressure-density gradients force the land air mass seaward, the marine air is lifted, carrying the prevailing wind aloft with it. The undercutting land breeze is thus producing strong vertical shear. The surface is dominated by a gentle negative u velocity wind field while the winds aloft are probably still strongly negative v. The influence of the negative v winds is greatest where the penetration of the land breeze is weakest, such as at S4 and S5.

The decay of the land breeze begins at sunrise, about 0530. All stations experience a local temperature increase which in a matter of two hours raises the air temperature back up to its daytime range. By 0800 the steep land-sea temperature gradient has been replaced by a shallow daytime gradient, and the pressure-density solenoid that drove the land breeze vanishes. At this time the land breeze wind speed minimum still persists at all stations; not until the air temperature has returned to its daytime value does the wind speed begin its increase. It is a gradual process. Whereas the land breeze dropped the wind speed in a period of about two hours, it will take six hours for the wind speed to regain its daytime maximum. Apparently we are not seeing a sea breeze frontal return flow; instead it seems that the displaced prevailing wind field errodes the low velocity surface air mass from above. There is no progressing return that would be indicative of a front, the wind speed increase occurs almost simultaneously over the array. By early afternoon the low velocity air is gone, the prevailing southward wind has resumed its position along the shore, and the stage is set for another land breeze.

Event II displayed the same general features as the first event, but contained some interesting variations. The temperature gradients (Figure 8b) were steeper than before and extended farther offshore, but the negative u velocities were only slightly greater than those for

Event I. Station S1 displayed an unusual four hour delay between the decrease in wind speed at 1800 and the sharp temperature drop at 2200. This perhaps is due to a slight veering in the coastal wind, so that S1 is shielded by the surrounding bluffs from the wind. The land breeze apparently arrives at 2200 along with the cooler air. At the other stations the wind speed and temperature decrease simultaneously. S2 experienced a very dramatic decrease in wind speed of 5 m/sec, with a temperature drop of 1° C in the space of half an hour. The decreases were not so rapid at the other stations, but were generally more distinct than those observed on the previous night. The land breeze front was very ragged at S3 and S5 on the north side of the array, while the southern stations S2 and S4 exhibited sharper decreases; the separation between the north and south sides of the array is only 6 km.

If we assume that the land breeze arrived at S1 at 2200, then the timetable for this event is very similar to that of the first event. Arrival times: S1 at 2200, S2 at 0100, S3 at almost 0300, S4 and S5 at 0400. Recall that during Event I the breeze was at S1 at 2300 and appeared at S4 and S5 at 0500. The progress of the front is surprisingly consistent between the two nights; although it begins an hour earlier in Event II, it still requires about six hours to cover the 14 km of the array. The record ends at 1120, but we can see that the

dawn reversal of temperature occurred as before and that again the wind speed did not begin its increase until two hours later at 0800.

In spite of their differences the two events are remarkably similar. Is such similarity normal or were these events unusual twins? We shall encounter more similarities in the divergence and vorticity records, but it still seems strange that the processes which produced the events should be so stable in such a turbulent coastal regime. What accounts for the stability--the pressure field, the sea temperatures, the amount of solar radiation? The land breeze does not leave the shore until some three or four hours after sunset. Presumably this is the amount of time necessary for cooling to produce a gradient that can accelerate the air mass against the retarding surface friction. Is this cooling time a constant, or is it a function of the temperature field and the terrain involved? A related question is why is there a two hour lag between the dawn increase in temperature and the 0800 wind speed increase? Since the lag occurs simultaneously over the array it doesn't seem to be related to a front overcoming friction, but then, what determines the duration of the lag and how constant is it? Clearly, further investigation of the land breeze is necessary before a model can be formulated that will answer all these questions.

The progressive vector diagrams (PVD's) presented in Figure 9 demonstrate how strongly the vector diagrams are affected by the

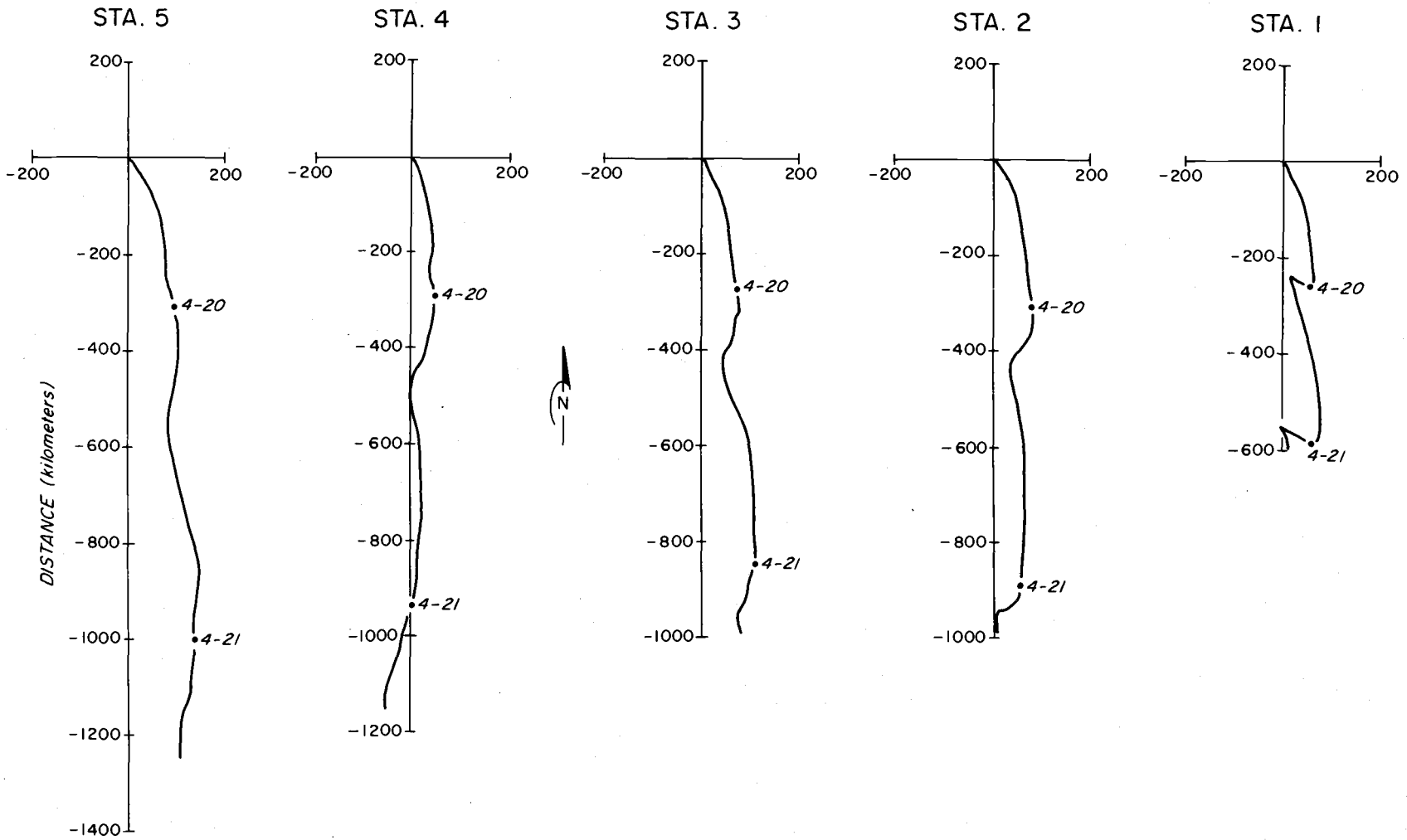

Figure 9. Progressive Vector Diagrams.

land breeze. For this case of a prevailing southward wind, the land breeze events form a distinct westward hook in the diagrams when they arrive at the various stations. Since the land breezes are generally weak, and their presence may be difficult to notice in time series of temperature or wind velocity, the use of PVD's could facilitate their discovery, especially in long records of data.

In conclusion we mention that the sea temperatures plotted in Figures 3 through 7 are mostly identical--values of 10° C cover most of the record and with only two exceptions the water temperature is always at least a degree centrigrade warmer than the air temperature. This explains why the air temperature over the water is so stable--a thermal gradient exists so that heat is constantly flowing from the water into the air. The two exceptions occur at S2 and S3. The air temperature at S3 agrees with S4 and S5 during the night, but is anomalously high in the sunlight, raising a few degrees above the sea water temperature. This is probably due to a faulty radiation shield around the sensor probe which allowed the probe to be heated directly by the sun instead of measuring air temperature. The sea temperature at S3 agrees with S4 and S5. At S2 we see an anomalously low sea temperature: generally less than 6° C and even dropping to 3.5° C at one point. These are arctic sea temperatures--even during Oregon upwelling the sea temperature seldom goes below 8° C.

Unfortunately, the author has not been able to explain the low temperatures as an equipment malfunction although it must be in error.

Divergence and Vorticity

With the use of buoys and automated, meteorological data recorders, we are able to make mesoscale measurements that have previously been impossible or impractical. Little is known about the behavior of the mesoscale divergence and vorticity fields because overland the measurements require complicated elevation corrections (Schaefer, 1973) and are strongly affected by microscale inhomogeneity in the wind fields (Mahrt, 1974). Oversea widespread simultaneous observations have been difficult to make. However, the ocean is the ideal place to study wind field structure, because of the constant, sea-level elevation and the lack of terrain obstructions. Cummings (1973) provides us with some of the first measurements of oceanic mesoscale horizontal divergence and vertical vorticity from a month in the North Atlantic during the Joint Air-Sea Interaction study, JASIN. Using the same equipment and approach, we can now investigate the response of the mesoscale wind field to a known input: the land breeze.

Cummings (1973) describes in detail the techniques and the programs used to compute the divergence of the horizontal velocity field, and the vertical component of vorticity. He lists two programs,

DIVCONV and VORT, which perform the calculations. The author has modified Cummings' divergence program DIVCONV so that it will compute both divergence and vorticity over a polygonal array using simplified inputs. The new program is called DIVORT and is listed in the appendix. The method it employs in its calculations is described below. (A similar approach is used by Graham, 1953.)

An observational polygon is formed by buoys each equipped with wind velocity sensors, clock and data logger. Simultaneous records from all the buoys is thus obtained. The simultaneous wind velocity vectors from two adjacent vertices of the polygon are used to compute an averaged wind vector for the side of the polygon between the two vertices. This average vector is then analyzed into a component normal to the side and a component tangent to the side. The procedure is followed for the other sides of the polygon until each side has a normal and tangential vector representing the average wind velocity for that side. The area of the polygon and the lengths of all the sides are known.

Figure 10 shows a triangle with the side vectors added. To compute divergence, we use Gauss' Theorem:

$$\int \vec{\nabla}_H \cdot \vec{V}\, dVol = \int \vec{V} \cdot \vec{n}\, da \,. \qquad (1)$$

$\vec{V}$ is the velocity field under examination, $\vec{V} \cdot \vec{n}$ is the normal component of $\vec{V}$ on a face with area da. $\vec{\nabla}_H$ is the horizontal del operator,

$$\vec{\nabla}_H = \frac{\partial}{\partial x}\hat{i} + \frac{\partial}{\partial y}\hat{j} \,,$$

so that $\vec{\nabla}_H \cdot \vec{V}$ represents the horizontal divergence:

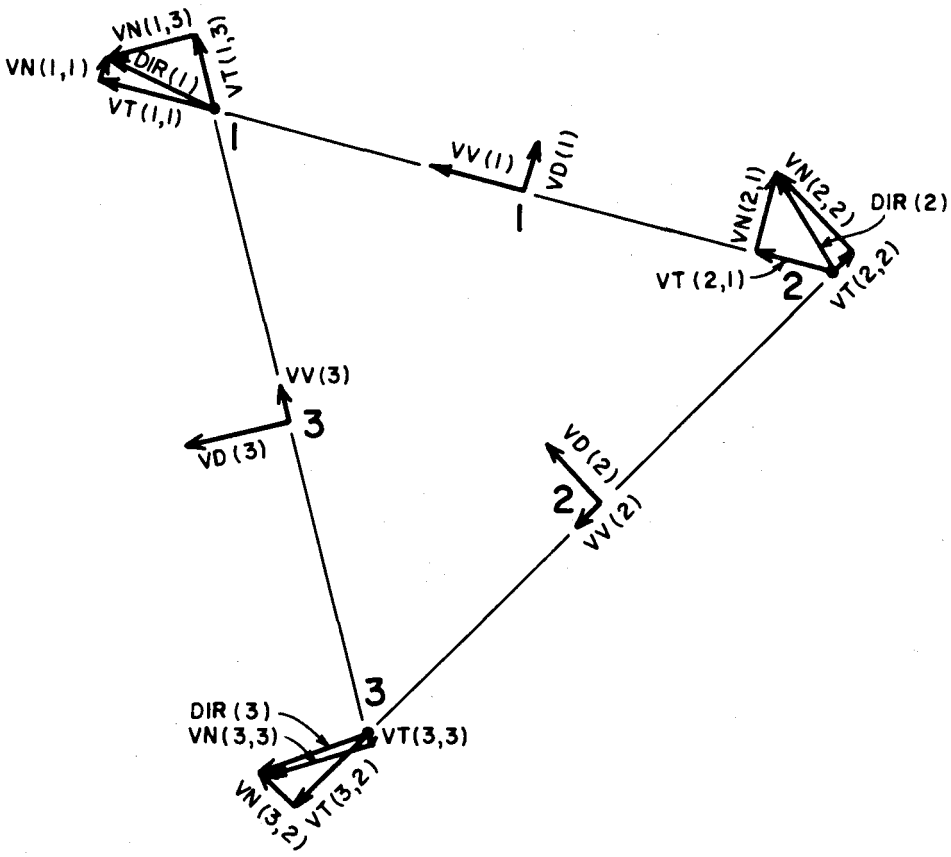

Figure 10. Hypothetical Buoy Array for Computation of Divergence and Vorticity Using DIVORT.

$$\vec{\nabla}_H \cdot \vec{V} = \frac{\partial u}{\partial x} + \frac{\partial v}{\partial y} . \tag{2}$$

The integral on the left in (1) is taken over the volume of the polygon; for a polygon with area $\underline{A}$ and for buoys with a height $\underline{h}$, the volume is just $\underline{Ah}$. The area of a face of the polygon is the length of the side $\underline{L}$ times the buoy height $\underline{h}$, or $\underline{Lh}$. For a polygon with n sides we can approximate (1) with

$$(\vec{\nabla}_H \cdot \vec{V})Ah = \sum_{i=1}^{n} Vn_i \, L_i \, h \tag{3}$$

where $\underline{Vn_i}$ is the normal component of the velocity for face $\underline{i}$. This simplifies to

$$\vec{\nabla}_H \cdot V = \frac{\sum_{i=1}^{n} Vn_i \, L_i}{A} , \tag{4}$$

so that it is not necessary to specify the height of the buoys, $\underline{h}$.

Stoke's Theorem is used to compute the vorticity. The theorem is

$$\int (\vec{\nabla}_H \times \vec{V}) \, dA = \oint \vec{V} \cdot d\vec{l} . \tag{5}$$

Here $\underline{d\vec{l}}$ is an infinitesimal length vector on the perimeter of the polygon and the circuit integral is taken counterclockwise around the polygon for positive values. As before, we can approximate (5) for an $\underline{n}$-sided polygon with

$$\vec{\nabla}_H \times \vec{V} = \frac{\sum_{i=1}^{n} Vt_i \, L_i}{A} , \tag{6}$$

where $\underline{Vt_i}$ is the tangential component of the velocity for side $\underline{i}$. This computes the vertical component of vorticity, or

$$\hat{k} \cdot \vec{\nabla}_H \times \vec{V} = \left(\frac{\partial v}{\partial x} - \frac{\partial u}{\partial y} \right) \quad . \tag{7}$$

The simple forms of (4) and (6) allow both divergence and vorticity to be computed quickly with no other inputs than the wind velocity vectors, the area of the polygon, the lengths of the sides, and the angle between true north and the outward normal vectors for each side (the frame of reference is relative to true north). Moreover, once the horizontal divergence is known, the verticle flow out of the polygon can be computed from the continuity equation:

$$\frac{\partial u}{\partial x} + \frac{\partial v}{\partial y} + \frac{\partial w}{\partial z} = 0 \ . \tag{8}$$

Substituting (2) into (8) we get

$$\vec{\nabla}_H \cdot \vec{V} = -\frac{\partial w}{\partial z} \ . \tag{9}$$

By integrating (9) from z=0 to the height of the buoy, $\underline{h}$, we get

$$w(h) - w(0) = - \int_0^h \vec{\nabla}_H \cdot \vec{V} \, dz \ . \tag{10}$$

It is assumed that $w(0) = 0$ (i. e., neglecting tidal and other changes in sea level), so that we can approximate (10) with

$$w(h) = -(\vec{\nabla}_H \cdot \vec{V}) h \tag{11}$$

Thus, to compute the vertical velocity, $\underline{w}$, out of the polygon, the horizontal divergence is simply multiplied by $-\underline{h}$.

As the land breeze moves seaward we can expect to see a zone of convergence where the marine air is lifted by the colder land air. Various numerical models of sea-land breezes predicit the zone and it has often been observed from bands of cumulus clouds (produced by moist, rising air) or experienced during soaring flights. Hsu (1970), in his model for the Texas coast, with no prevailing wind, predicts a convergence zone for the land breeze 30 km offshore. During a land breeze in Texas, Eddy (1966) reported seeing an offshore band of cumulus clouds at dawn, which cleared rapidly after sunrise. He did not report how far offshore the clouds were, but it is assumed they were within 10 km of the shore.

Figures 11, 12 and 13 present the time series plots of divergence for each of the equilateral triangles formed by the buoy array. Beginning with the two triangles closest to shore, C and B, we see that the divergence shows little variability over most of the record, but is strikingly affected by the land breeze events. Event I produces a divergence peak in both B and C at 0200 which falls quickly to a period of steady convergence lasting until 0500. This apparently is the expected convergence zone. Event II produces a similar reaction in triangles B and C. The divergence peak occurs just after midnight. The period of convergence lasts until 0700 and is generally weaker and more variable than the zone in Event I.

It appears that the approach of the convergence zone is heralded by a divergence peak. This peak occurs during both events in both

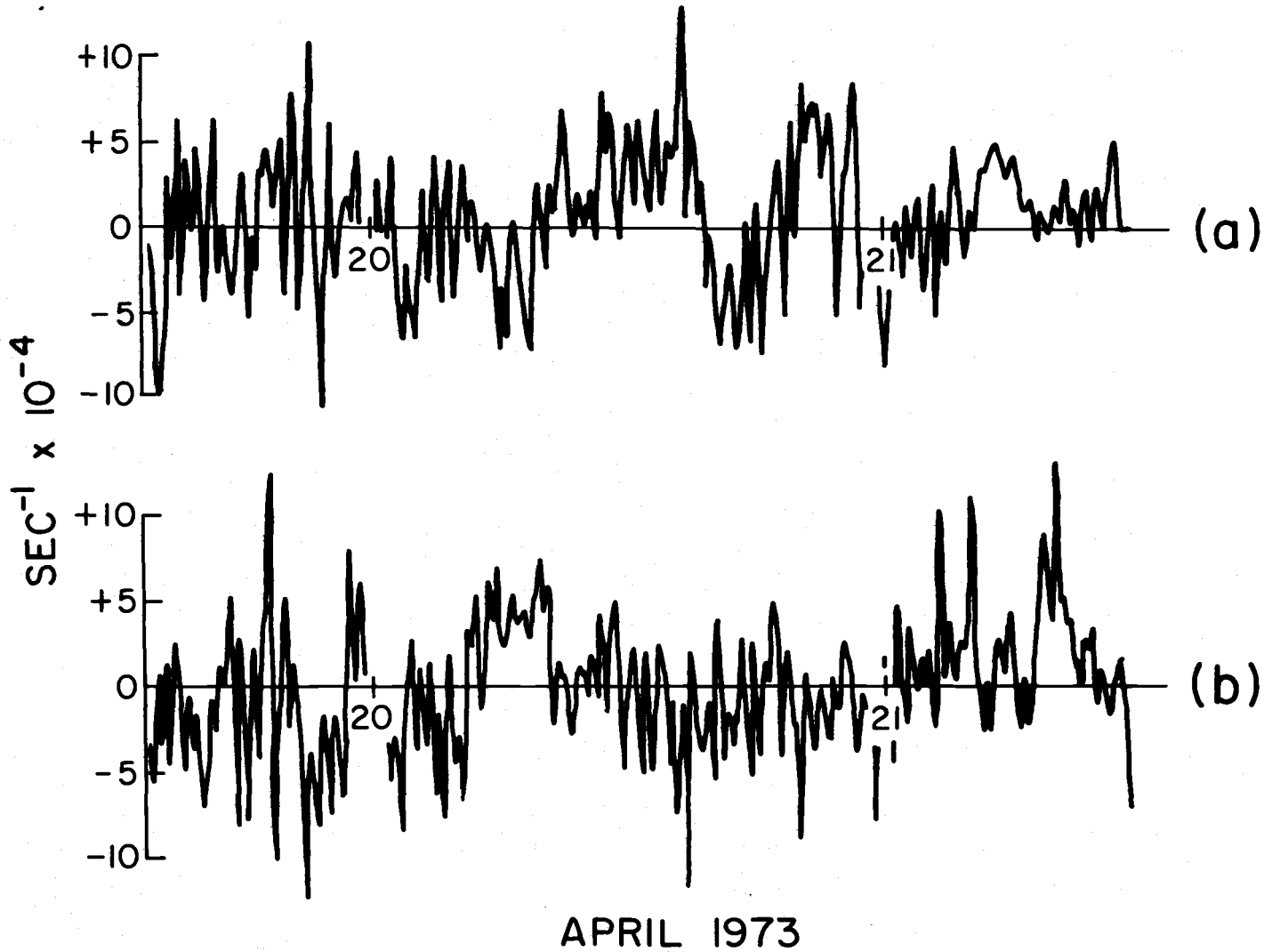

Figure 11. Triangle A (a) Divergence (b) Vorticity.

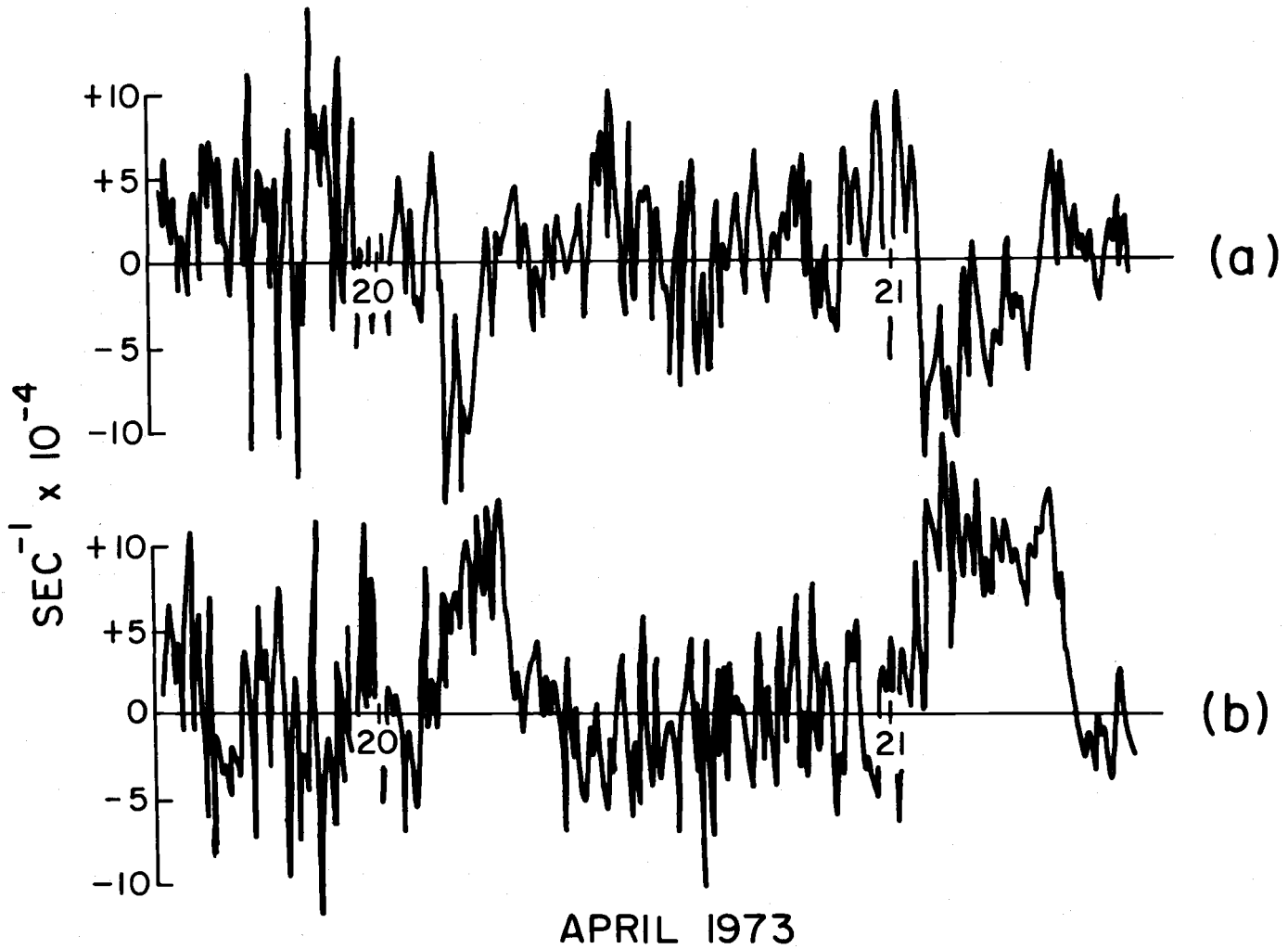

Figure 12. Triangle B (a) Divergence (b) Vorticity.

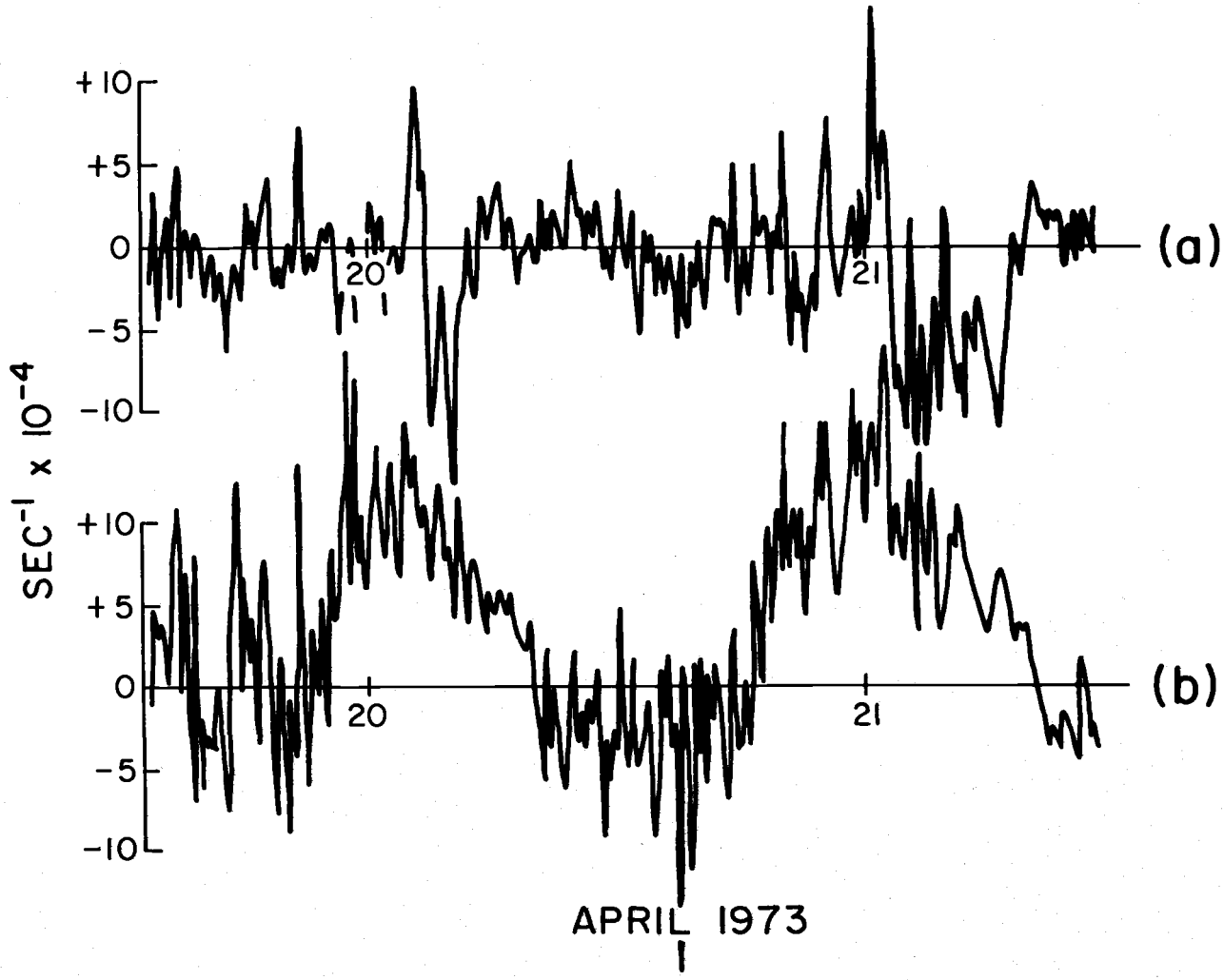

Figure 13. Triangle C (a) Divergence (b) Vorticity.

triangles and is assumed to be a regular feature of the land breeze front. Since few mesoscale measurements have been made of atmospheric phenomena, it is not known whether this pattern of divergence-convergence has been observed before in relation to sea-land breeze fronts. Wallington (1959, 1965), during a glider flight in England, reported encountering a region of downdraft just preceding the intense updraft of a sea breeze front. Presumably the convergence draws in air from in front of it, thus creating a small region of sinking air and diverging surface winds before it.

The record from triangle A supports the conviction that these land breeze convergence zones are located within 10 km of the coast. The periods of intense convergence are conspicuously absent. In their place, however, is something highly intriguing. From 0300 until 0500 on the 20th, during the time that Event I is producing its strongest convergence in the near shore triangles, there appears an unusual set of alternating divergence and convergence peaks in A. Each peak is of roughly the same intensity, the spacing between two divergence peaks, or two convergence peaks, is a regular period of 40 minutes. Event II has a similar set of peaks starting at 0100 and lasting until about 0400 on the 21st. Again, this corresponds to the time of maximum convergence in B and C. The peaks in Event II are more irregular, but once more the 40 minute period can be observed.

This form of periocity does not appear at any other times in any of the triangles. These features shall be investigated more in Section IV, to examine the author's contention that they are evidence of horizontal roll vortices generated by the land breeze convergence zone.

One last oddity is the intense divergence that appears in A and B between 2000 and 2200 on the 19th. It is doubtful that these peaks are related to the land breeze which arrives five hours later. They do, however, occur at the same time as the two cold air spurts seen in the air temperature record for S3, S4, and S5. Apparently cold air is sinking over the array. It was mentioned in the section on air temperature that the source of the air seems to be farther north up the coast. The correspondence between the divergence and air temperature records is interesting and assist us in locating significant features of the mesoscale.

Before examining the vorticity record, let us check how well the intensities observed for divergence and vorticity compare with expected values. Petersen (1956) estimated the various divergence scales from their time scales. For variations on the order of 1 hour--subsynoptic--the divergence is on the order of 2×10^{-5} sec^{-1}. We can expect the same scales to apply to vorticity, since the same velocities and spatial variations are used. Haltiner and Martin

(1957), referring to Panofsky (1946) showed that divergence will be proportional to the inverse of the length scale of the array measured in meters. For our buoy spacing of about 7 km ($\approx 10^4$ m), we can again expect divergence and vorticity scales to be on the order of 10^{-4} sec^{-1}. Cumming's(1973) observations of two triangles with different length scales support this last contention. Now, typical values observed for the divergence during the April land breeze events are 9×10^{-4} sec^{-1} for the divergence peak preceding the front and -5 to -10×10^{-4} sec^{-1} for the convergence zone. The measurements made here agree fairly well with the expected values, although perhaps they are slightly larger due to greater than normal verticle motion during the land breeze convergence.

The vorticity record exhibits a span of positive vorticity in the nearshore triangles C and B during both events. The periods of positive vorticity in C correspond closely with the low wind speed record for S1, lasting from 2200 until 0800 for Event I and from 1900 until 0800 for Event II. The intensity in B is less than in C and the spans are shorter--Event I occupies 0200 to 0800 and Event II takes 0100 until 0800. In A there are only brief periods around 0600 to 0800 that could correspond to the land breeze.

The correspondence between positive vorticity and low wind speeds suggests that the vorticity is produced by the horizontal shear in the v-component of velocity during the events. From equation (7)

we see that vertical vorticity is composed of two terms, $\frac{\partial u}{\partial y}$ and $\frac{\partial v}{\partial x}$. Now, since the land breeze front's progress is normal to the shore, and, as we have seen, the v-component drops rapidly when the front arrives, we can expect the front to be long and homogenous in the y-direction but narrow and varying quickly in the x-direction, so that $\frac{\partial v}{\partial x} \gg \frac{\partial u}{\partial y}$. Thus,

$$\vec{\nabla}_H \times \vec{V} \approx \frac{\partial v}{\partial x} \approx \frac{\Delta v}{\Delta x} . \tag{12}$$

Using values from S1 and S5 taken at 0200 during Event I,

$$\frac{\Delta v}{\Delta x} \approx \frac{7 \text{ m/sec}}{14 \text{ km}} = 5 \times 10^{-4} \text{ sec}^{-1} .$$

This agrees well with the observed values for vorticity in B for Event I. If this explanation of the vorticity is correct, then the intensity and sign of vorticity during a land breeze will depend respectively on the strength and direction of the prevailing coastal wind. Thus, for a wind blowing north, negative vorticity would be produced. Evidence of negative vorticity during a convergence might be obtained in the winter months in Oregon, when the wind is generally out of the southwest. Such observations would help test whether the land breeze vorticity is produced by shear or some other mechanism. For example, positive vorticity may also be created by the conservation of absolute vorticity during the downhill descent of the land air mass as it moves seaward. Vorticity produced in this manner would be less than the planetary vorticity, or about 10^{-4} sec^{-1}. This would be

masked by shear vorticity when there is a strong prevailing wind, but could perhaps be observed during periods of calm. Clearly, more investigation of the land breeze is required to make a reasonable model for land breeze divergence and vorticity.

IV. HORIZONTAL ROLL VORTICES

It was mentioned in the previous section that although triangles B and C experienced a period of convergence during the land breeze, in Triangle A the convergence zone was absent. Instead we saw alternating peaks of divergence and convergence with a period of about 40 minutes. After a closer examination of the data plots, it was discovered that similar fluctuations occurred in the u-component time series for S5 and S3, and less dramatically at S4. The best model the author could find to explain these unusual features is that of horizontal roll vortices induced by the land breeze convergence zone. If this belief is confirmed, this will be the first time that roll vortices have been observed in a sea-land breeze front, which in turn may indicate that these rolls are in best agreement with the buoyancy-parallel vertical shear theory of roll production.

Horizontal roll vortices are durable, helical movements of air that occur in the Planetary Boundary Layer (PBL) of the atmosphere during slightly unstable conditions with moderately strong winds. They are important features--the subject of much current research--because it is believed that they profoundly influence the distribution of heat and moisture throughout the PBL (Tennekes, 1974). The structure of rolls is still unclear, but they seem to resemble the schematic in Figure 14. In words, they are counter-rotating vortices,

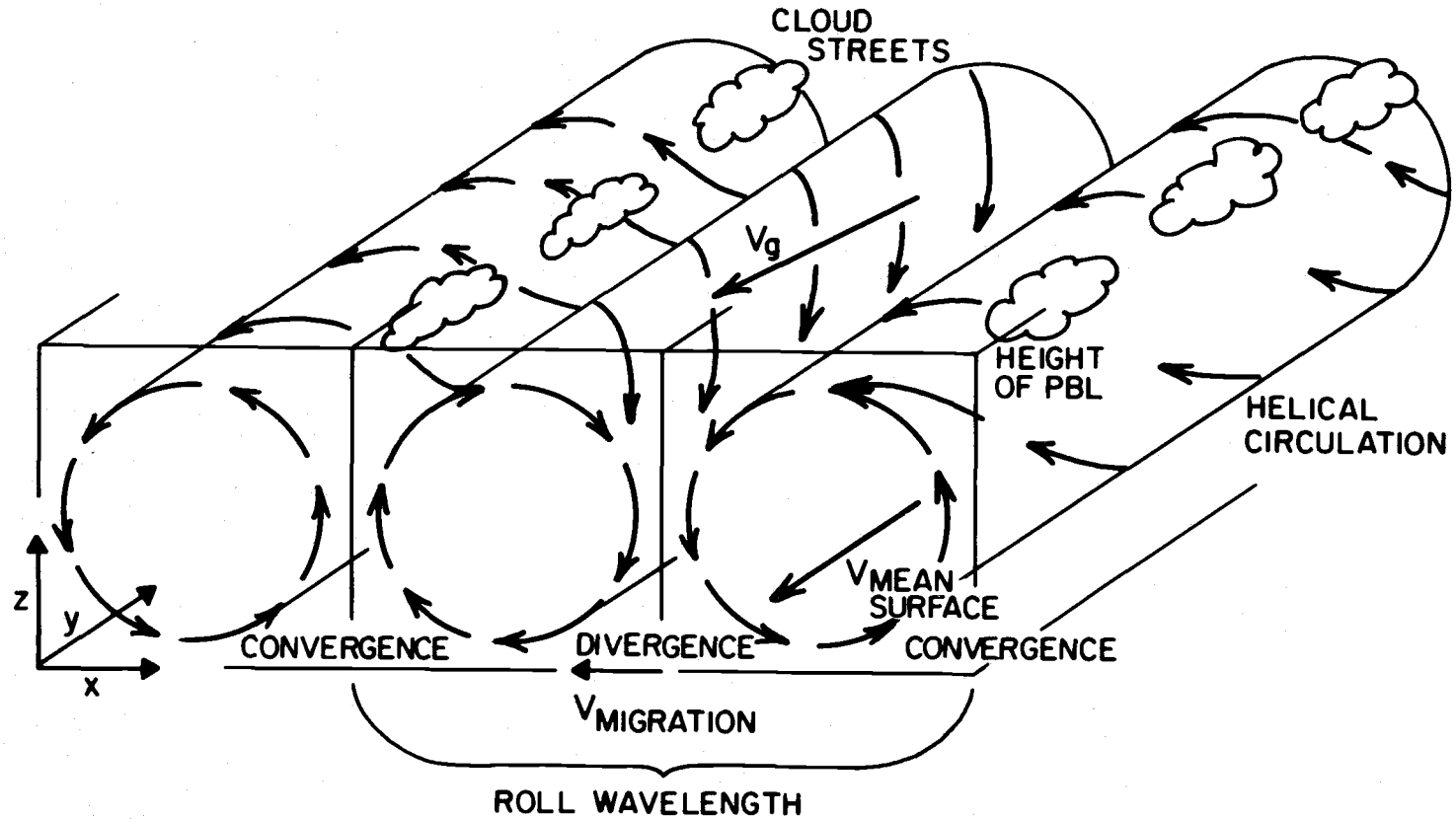

Figure 14. Schematic of Horizontal Roll Vortices.

with axis aligned along the mean wind direction. From observation and theoretical considerations, the roll width (wavelength) is about three times the height, which is roughly equal to the height of the PBL. Between the individual rolls there is a zone of divergence or convergence, depending on the direction of rotation of the adjacent rolls. Roll convergence zones often produce cumulus clouds which are, since they are created in long, parallel bands, the familiar "cloud streets" sometimes seen during periods of fair weather and strong winds. An interesting feature of roll vortices is that they "migrate" in the cross wind direction. For example, if a fairly strong wind is blowing south, rolls will form along a north-south axis and then slowly migrate either to the east, or, to the west.

Satellite photographs reveal that cloud streets are a very common feature of the Earth's troposphere. From studies of the photographs by Kuettner (1971) it was determined that the street spacing is 2 to 8 km and that the bands can be up to 500 km in length. However, the roll vortices are also known to occur without producing cloud streets. One of the earliest observations was that of Woodcock (1942), who noticed that seagulls can soar in straight lines along the wind direction when the sea is warmer than the air and the wind is strong. He concluded that the gulls were benefiting from "longitudinal roll convection cells" that had been observed in laboratory experiments with thermally convecting fluids. Another clear air observation of

rolls was made by Angell, et al. (1968), who released baloons in the PBL and followed their helical trajectories on radar. The most thorough investigation of rolls to date has been made by LeMone (1973). She uses data from a TV tower array in Oklahoma and NCAR flights over the Great Lakes to determine the structure and energetics of roll vortices. Her findings concur with Kuettner about the dimensions of the rolls--wavelengths (the distance between cloud street-convergence zones, or two divergence zones) of 1.5 to 6.5 km and roll length at least 10 times the width were observed. Except for Woodcock's seagulls and satellite photographs, investigations of roll vortices have been made over the continents and they have not been studied at sea.

LeMone investigated rolls as they migrated over her array. She reports that it took from 30 minutes to an hour for one to pass over a fixed point. What this means is that it takes 30 minutes to an hour for two successive cloud streets to pass over, and, remembering that the two cloud streets are above convergence zones that are separated by a divergence zone, we see this implies that in less than an hour there will be a procession of convergence-divergence-convergence over the array. Angell, et al., found evidence that their helical structures moved in a direction normal to the mean wind at about 1 m/sec. If the distance between two convergence (or divergence) zones is 2 km (LeMone's horizontal roll wavelength), then it

will take 33 minutes for two successive convergence zones to pass over. Thus, if 2 km rolls are migrating at 1 m/sec, an array of surface wind sensors will experience a 33 minute periodicity in divergence and convergence.

During the passage of a roll the surface wind should change in response to the helical circulation around the roll. This is illustrated in Figure 20. If the roll axis is along the y-axis, then the most noticeable change will occur in the cross wind u-component. The u-component at a point will be positive if immediately east of it there is a north-south aligned convergence zone. Similarly, u will be negative if there is a divergence zone to the east. As the rolls migrate, the u-component will fluctuate at the same frequency; for example, it will have the same sign every 33 minutes for the above case. Notice that at a given point the u-component record and the divergence record will be 90° out of phase. We now continue with our examination of the station data collected during April, 1973. Evidence for roll vortices comes from two sources: the 40 minute periodicity in the divergence record for Triangle A and the behavior of the u-component of wind velocity at S5 and S3. Spectral analysis will assist us in determining the periodicity and coherence of these source records, and hence the validity of the evidence.

Figures 15 and 16 show the autocorrelation and the power spectral estimates for divergence in A during Event I and Event II. The

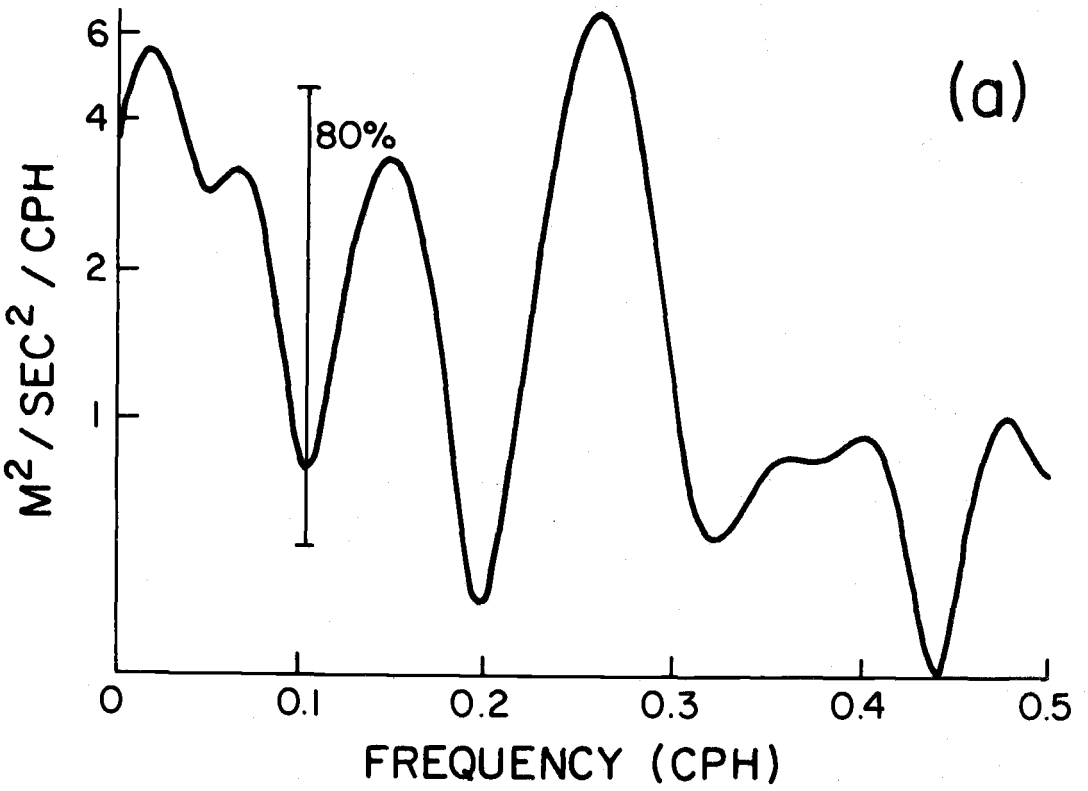

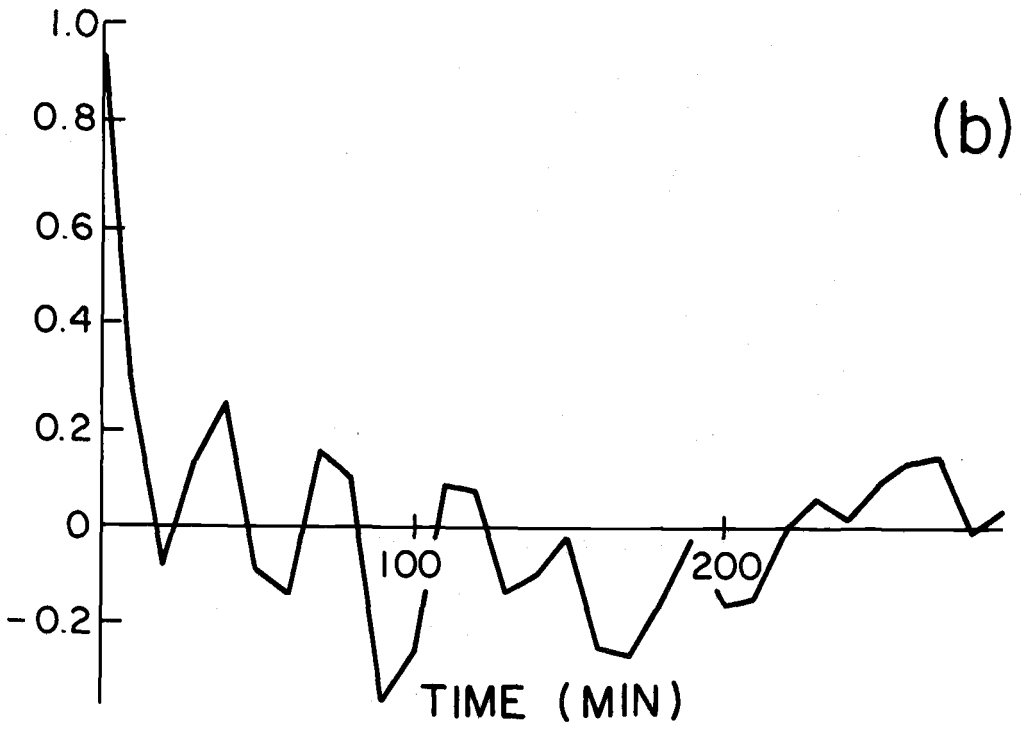

Figure 15. Divergence in Triangle A During Event I. (a) Power Spectra (b) Autocorrelation.

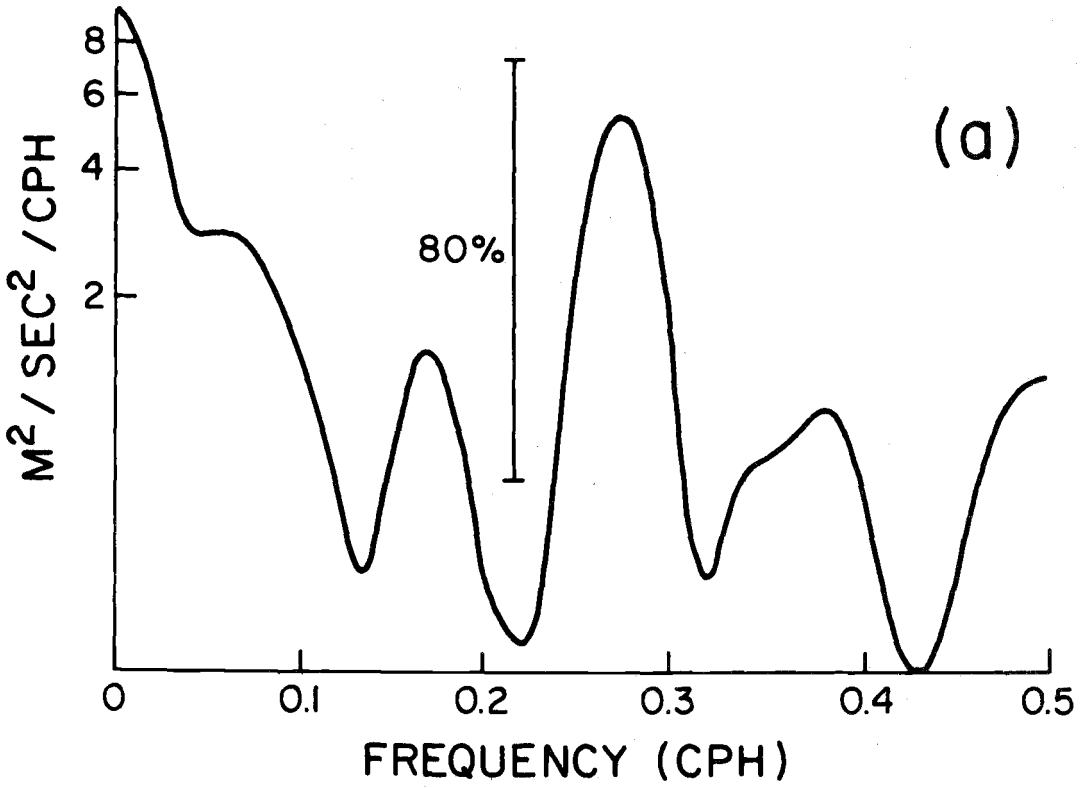

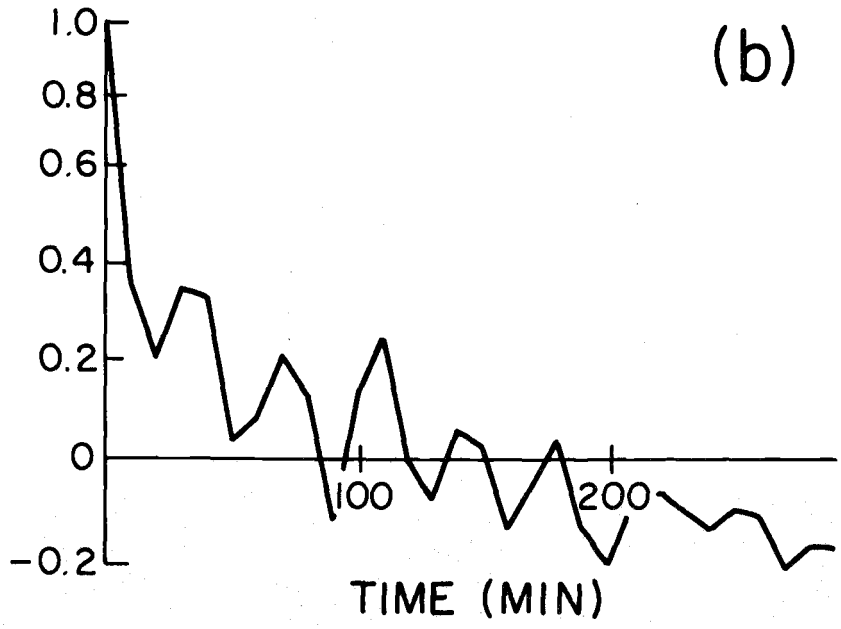

Figure 16. Divergence in Triangle A During Event II. (a) Power Spectra (b) Autocorrelation.

plots were made from 6 hours of data corresponding to the land breeze, from 0200 until 0800 for Event I and from 000 until 0600 for Event II. The programs and subroutines used in making these and the other spectral plots come from the OS-3 ARAND System; in this case, program SPECT2C was used (Ochs, et al., 1971).

We see in each power spectrum a significant peak at about 0.27 cph. This translates to a period of 38 minutes for Event I and 36 minutes for Event II. This then is the "40 minute" periodicity observed during the events. The only other significant peak is around 0.16 cph, which corresponds to a 63 minute period. The origin of this hourly fluctuation is unknown. In each case the 40 minute peak is about twice as high as the hourly peak.

The autocorrelation plots show that each record correlates with itself every 40 minutes. The hourly and other low frequency peaks appear, but again they are smaller than the main 40 minute periodicity.

Thus it appears that divergence-convergence bands are moving over Triangle A every 36 to 38 minutes, which agrees very well with the 30 minutes to an hour spacing observed by LeMone.

Next, let us analyze the data for the three stations which form Triangle A--S3, S4, and S5. We will look at the u-component of wind velocity, which should be most strongly affected by north-south oriented rolls. Figures 17 through 19 present, for each station,

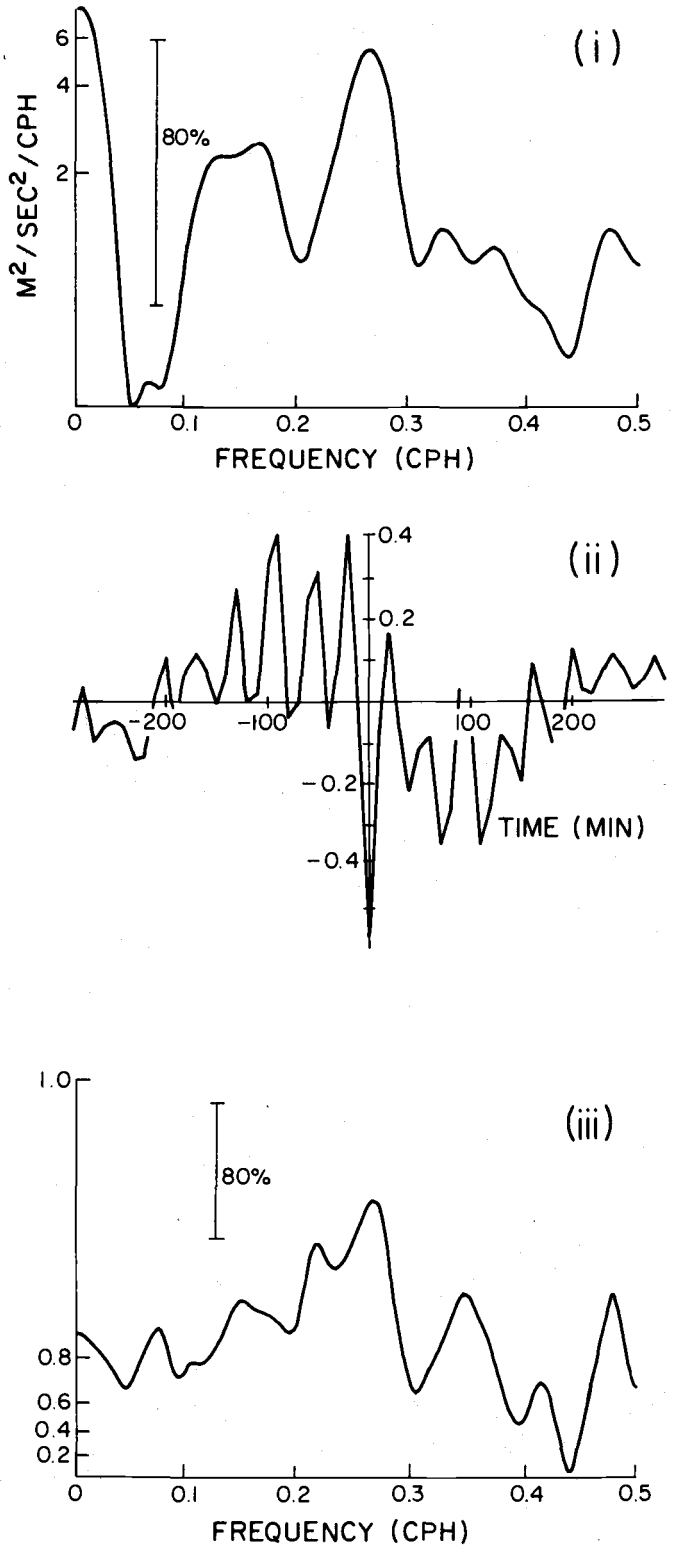

Figure 17a. Station 5 U-Component, Event I. (i) Power Spectra, (ii) Cross Correlation and (iii) Coherency with Divergence in A.

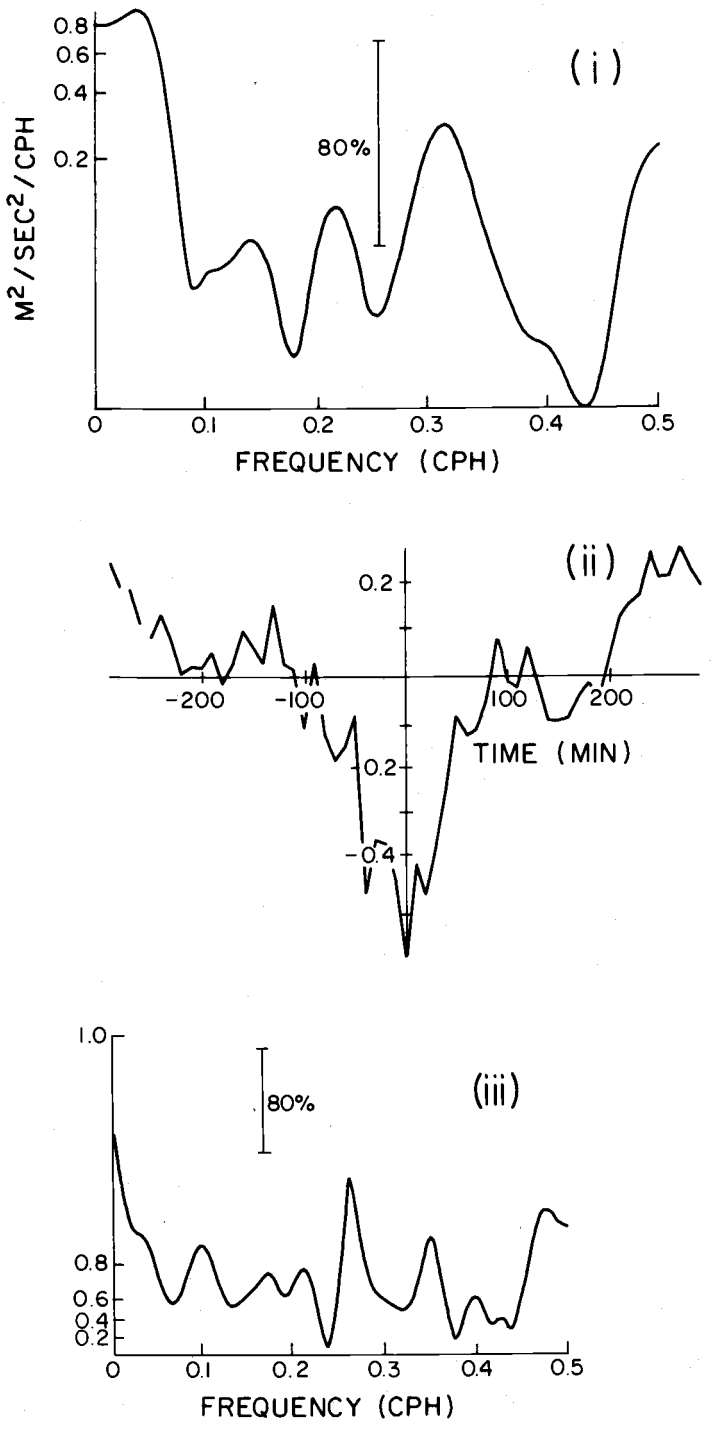

Figure 17b. Station 5 U-Component, Event II. (i) Power Spectra, (ii) Cross Correlation and (iii) Coherency with Divergence in A.

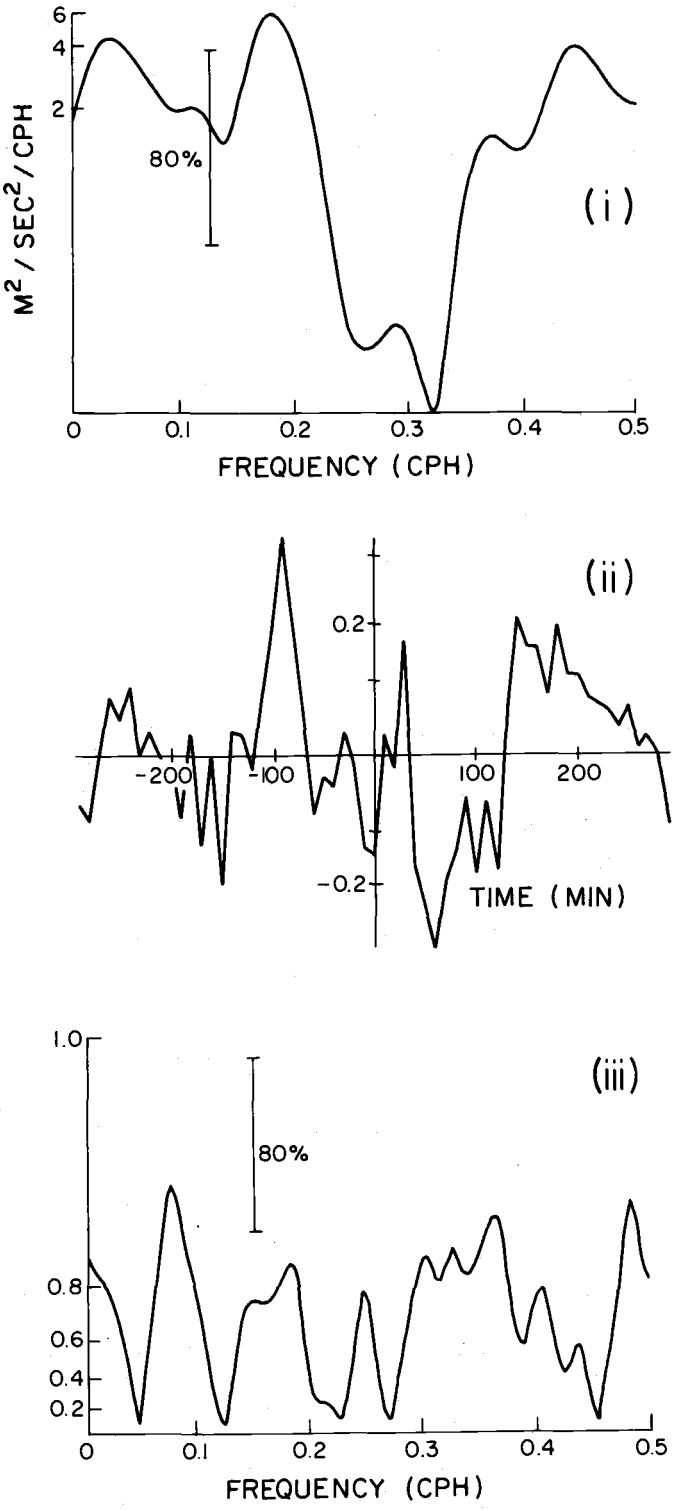

Figure 18a. Station 4 U-Component, Event I. (i) Power Spectra, (ii) Cross Correlation and (iii) Coherency with Divergence in A.

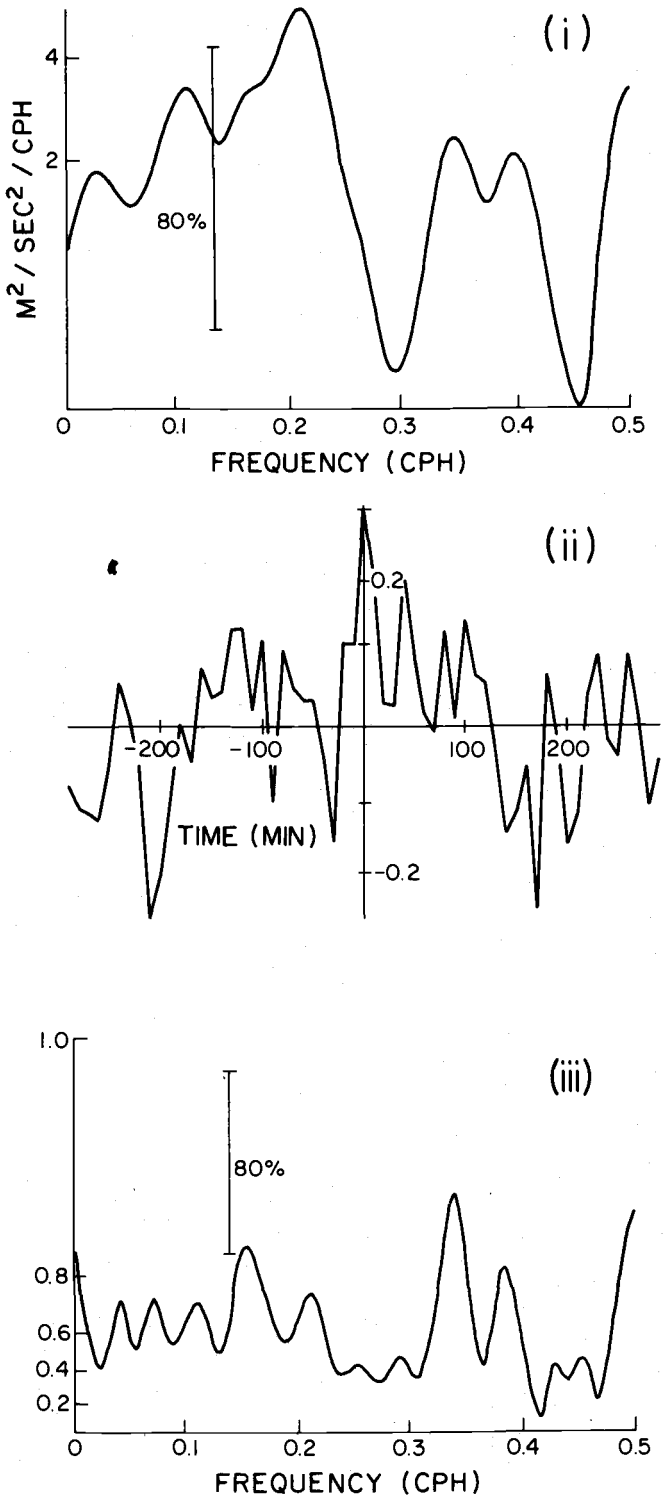

Figure 18b. Station 4 U-Component, Event II. (i) Power Spectra, (ii) Cross Correlation and (iii) Coherency with Divergence in A.

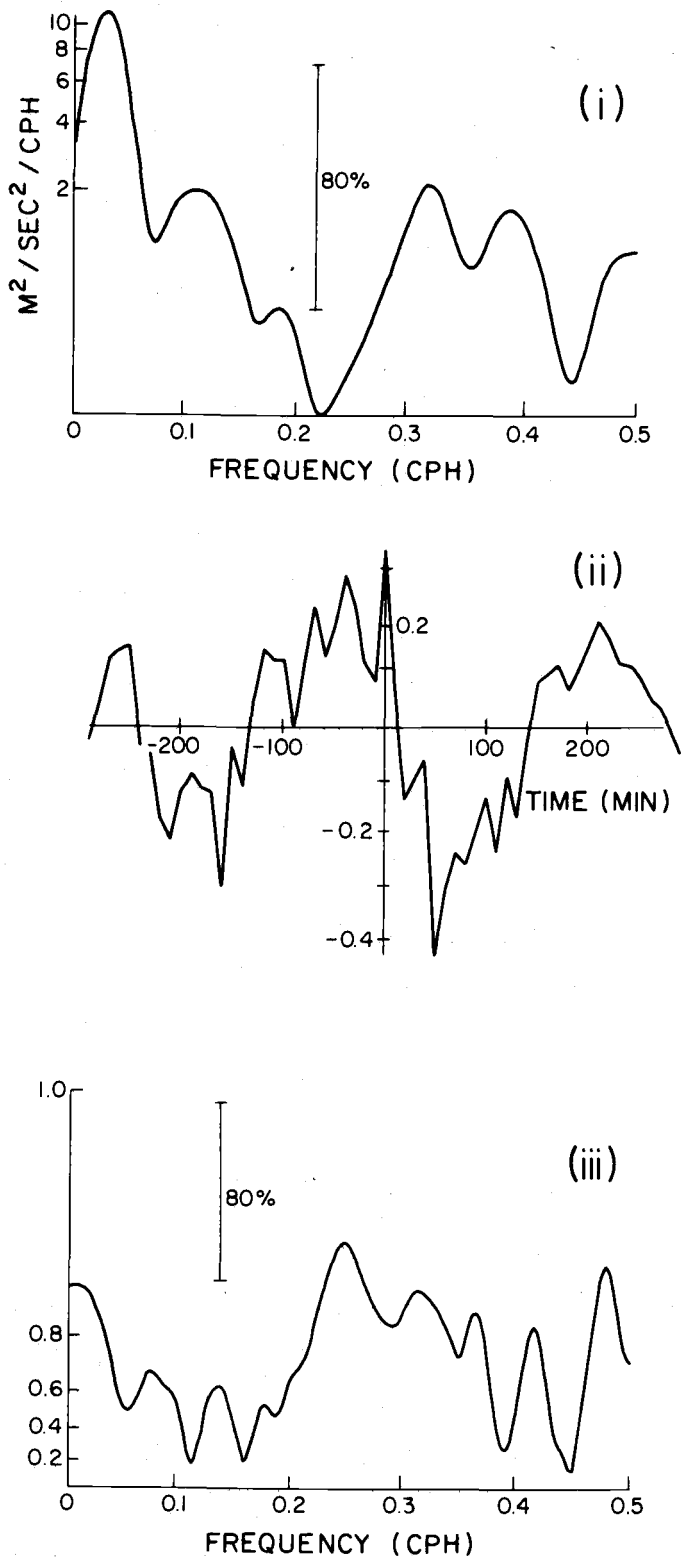

Figure 19a. Station 3 U-Component, Event I. (i) Power Spectra, (ii) Cross Correlation and (iii) Coherency with Divergence in A.

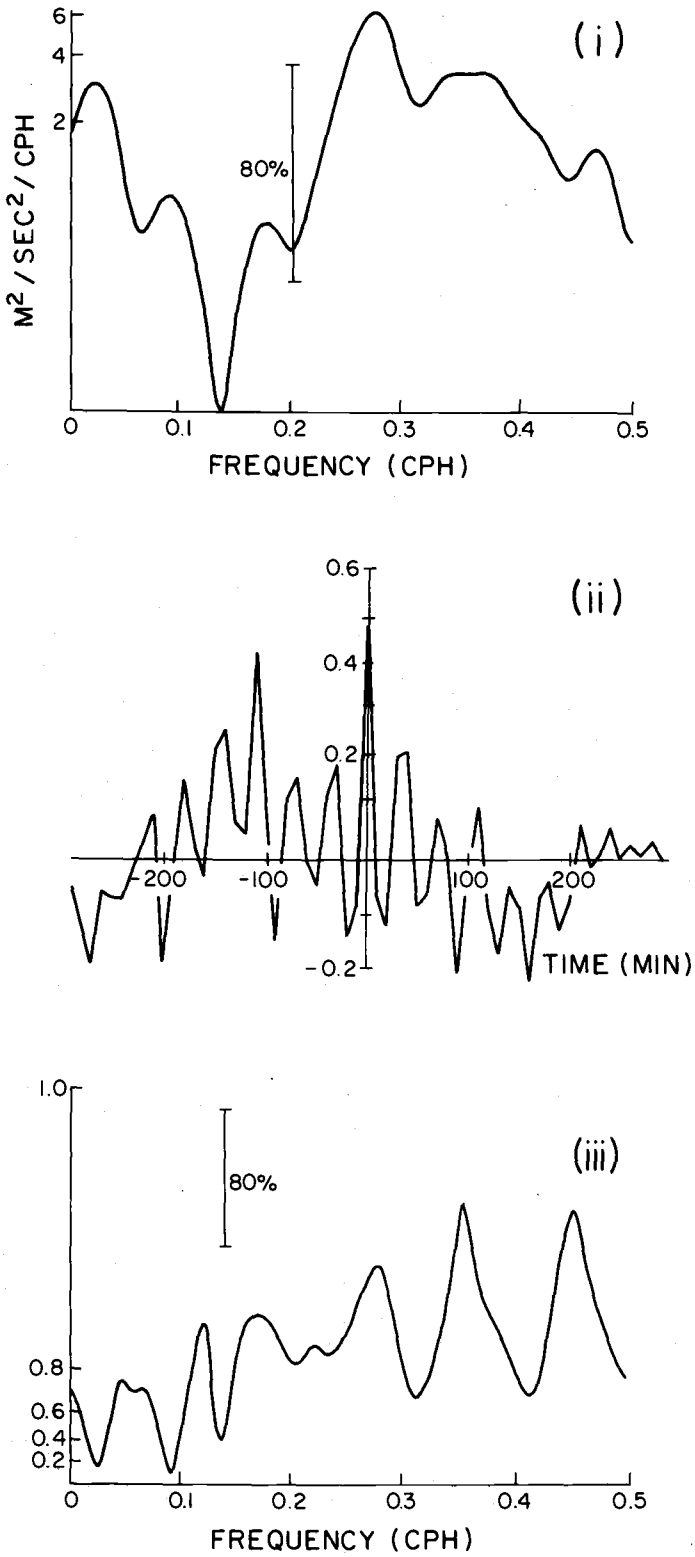

Figure 19b. Station 3 U-Component, Event II. (i) Power Spectra, (ii) Cross Correlation and (iii) Coherency with Divergence in A.

power spectral estimates, cross correlation with divergence in A, and the coherency estimates between u and divergence in A.

Beginning with Event I and S5 (Figure 17), we see from the power spectral plots that the u-component has a periodicity similar to the divergence in A. The main peak is at 0.27 cph--the 37 minute period--and again there is a smaller hourly peak. The plot of the cross correlation function shows how well the divergence time series and the S5 u-component time series line up with each other at different displacements of time. The main peak is at delta t (ordinate) = 0 and cross correlation coefficient (abscissa) = -0.61. This means that simultaneous record (delta t = 0) of the two series has strong negative correlation, i.e., one record has positive values when the other record has negative values. Thus, when Triangle A is experiencing convergence (negative values of divergence), the S5 u-component is positive (toward the east).

The final plot, coherency estimates at different frequencies, tells us at which frequencies do the two series show the greatest similarity (coherency). The peak here is at 0.28 cph, which corresponds to a period of 36 minutes. In summary, what all this says is that both the S5 u-component and Triangle A divergence have similar, prominent fluctuations with a period of about 36 minutes, but that the fluctuations are out of phase by 180° between the two series, so that when one series is positive, the other is probably negative.

By contrast the plots for S4 u-component (Figure 18a) show weak correlation with the Event I divergence in A. The main peak in the power spectra is down around 0.185 cph--54 minute period, perhaps the hourly peak. The cross correlation is low and negative at delta t = 0, but moderately large at delta t = -90 and + 60 minutes. The major peak in the coherency plot occurs at 111 minutes, and on the whole the coherency is very scattered. In summary, S4 u-component does not display the same periodicity that appeared at S5 and in the divergence in A. It does not show the strong coherency with divergence that was seen at S5.

S3 is only slightly better. Although the power spectrum (Figure 19a) plot shows nothing significant at 0.26 cph, the coherency plot does display good coherence around this frequency. The cross correlation predicts that divergence and S3 u-component will be in phase (positive for delta t = 0), and thereby S5 and S3 will be out of phase by about 180°.

Similar features for S3, S4 and S5 appear in Event II. An examination of the spectral plots reveals that

1) "40 minute" periodicity occurs in S5 and S3 (36 minutes at each station). There is a slightly smaller power spectral peak at S4 corresponding to a 44 minute period.

2) the cross correlation for S3 is strongly positive. At S5 it is strongly negative. The delta t = 0 peak is the greatest at each

station, with a magnitude of over 0.55. There is weak positive correlation at S4, the peak is not significant compared to peaks at different time displacements.

3) the coherency for S5 and divergence is greatest at 0.27 cph (= 37 minute period). S3 also has high coherency at this frequency but coherency is more prominant at higher frequencies. By comparison, the coherency at S4 is low with no peaks at 0.27 cph, although high frequency peaks, similar to those at S3, do appear.

Although the above findings seem rather complicated, many of the features can be readily explained by a simple horizontal roll vorticies model. Assume that roll vortices are migrating over triangle A as in Figure 20a. The dimensions and migration speed of the rolls are such that the periodicity of zones is the observed value of about 37 minutes. At the time when a convergence zone is centered over the triangle, the divergence record will have a large negative value. At the same time, S5 will be experiencing its maximum positive u value while S3 will feel maximum negative u. When the convergence zone is replaced by a divergence zone, the divergence value will be positive, the u-component at S5 and S3 will be negative and positive, respectively. Thus, the migration of rolls over the array causes 37 minute fluctuations in divergence and u-component of wind velocity and positive correlation between the sign of u at S3, but

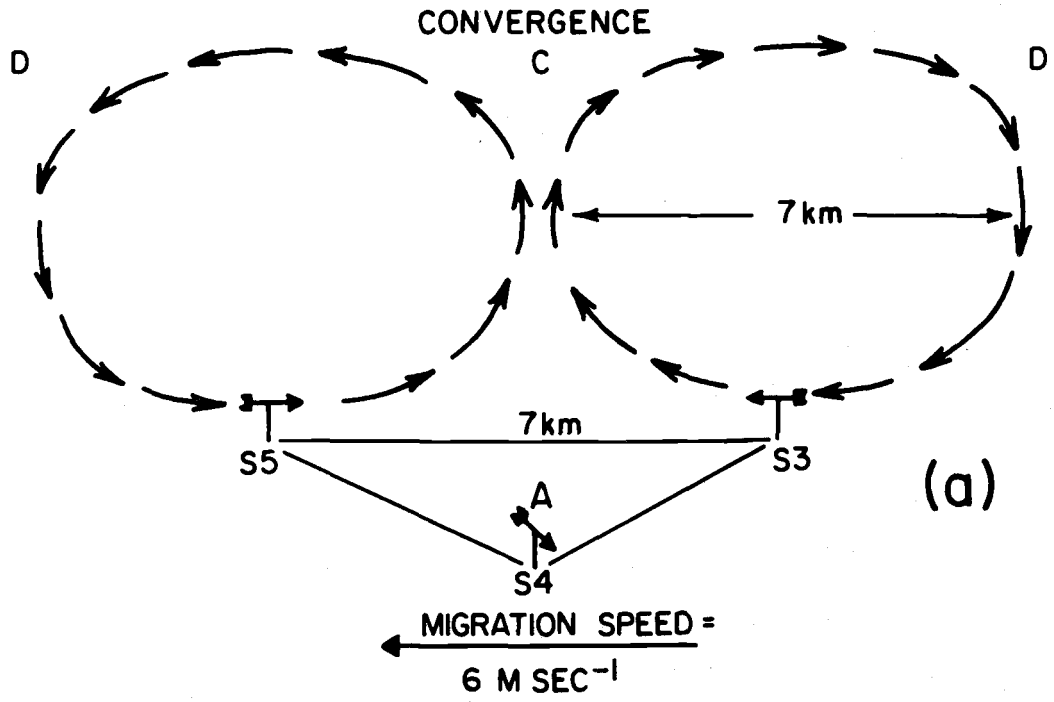

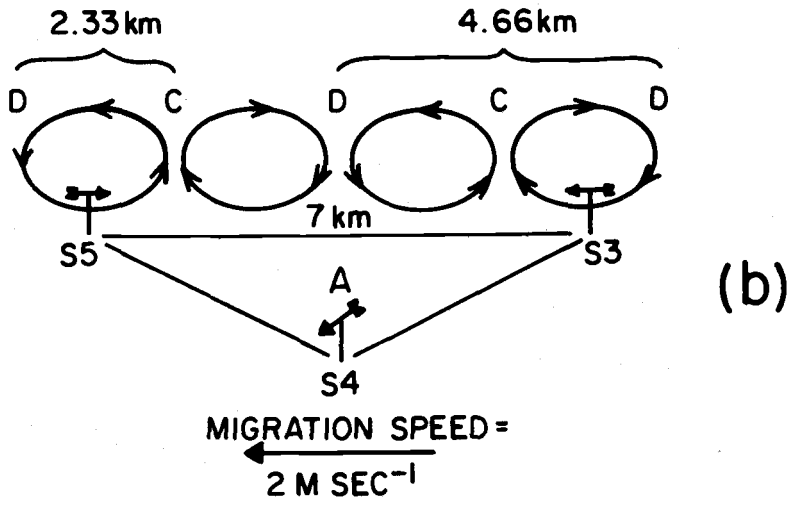

Figure 20. (a) Poor Model of Roll Dimensions
(b) Best Model of Roll Dimensions.

negative correlation between divergence and u at S5. These are the observed features during the two land breeze events.

From the dimensions of Triangle A we can determine the size of the rolls. If we use the model in Figure 20a, a single vortex will be about 7 km wide, thus the wavelength (i. e., distance between two similar zones) will be 14 km. This is rather large, the maximum wavelengths reported by LeMone was 6.5 km and by Kuettner was 8 km. Also, since the migration speed is the wavelength divided by the period, and since the period is 37 minutes, the migration speed must be 6.3 m/sec. This is much larger than the speed observed by Angell, et al. Clearly, this model is in poor agreement with previous findings.

However, excellent accord is achieved if we assume that there is more than one roll over the triangle simultaneously. The best model calls for four rolls and three alternating zones. (See Figure 20b). Now, from the dimensions of the array each roll is 2.33 km wide, so that the roll wavelength is 4.66 km, which is in good agreement with the known size of rolls. Dividing by the 37 minute period we get a migration speed of 2.1 m/sec. This too is more reasonable, and if it is true, then it suggests that rolls migrate faster over the oceans than over land. This would be expected from the smaller friction of the ocean surface.

The relationship between divergence and u-component still holds for this model. If one divergence and two convergence zones are over the array as in Figure 20b, then there will be a net value of negative divergence for the triangle. (In fact, the divergence zone is not "seen" by S3 or S5, whose velocities strongly determine the sign of the divergence over the array.) S5 will still experience positive u (negative correlation to divergence), and S3 will have negative u (positive correlation). Thus, the new model is in fine agreement with both previous observations of rolls and with the present findings.

How is it possible for the land breeze to produce horizontal roll vortices? The mechanisms of roll creation are still unclear, but there are two major theories to explain rolls. The first concerns thermal convection in moving fluids.

Laboratory experiments show that if a fluid at rest is heated from below, hexagonal shaped cells of convection will form. If the same fluid is moving in one direction and heated, longitudinal bands of convection in the direction of motion form instead (Scorer, 1958). In the PBL, the air is heated from below by heat stored in the land or ocean. The rolls that Woodcock observed occurred when the sea temperature was at least 3° C warmer than the air temperature and the wind speed was at least 8 m/sec. This suggested to Woodcock that the rolls were the bands of linear convection seen in the laboratory. Kuettner (1971) arrived at a similar explanation for rolls and described

a model whereby convection during periods of strong vertical wind shear will produce the horizontal rolls. Briefly stated, the increase of wind speed with height creates a vertical variation of horizontal vorticity which has high vorticity (strong shear in the vertical wind profile) near the ground and lower vorticity (weaker shear) with increasing altitude. If a parcel of air is displaced upward by buoyancy, the vorticity field will tend to return it to its original level. Thus, uplifting buoyancy forces must compete with vorticity gradient restoring forces. Kuettner states that the only way in which convection can arise is for all fluid elements along a horizontal line to rise simultaneously and circulate in a vertical plane normal to the horizontal axis. Therefore, horizontal roll vortices are formed which will make the vorticity field more homogeneous and will propagate new rolls.

The second theory of roll production indicates that rolls are a consequence of fluid motion over a rotating body, such as the Earth. As the wind moves over the rotating surface, an Ekman spiral attempts to form in the lower part of the PBL. By the nature of the spiral, there will at some point above the surface be a component of velocity in the direction normal to the mean wind. If the spiral is projected onto a plane normal to the wind, this cross wind component maximum will appear as an inflection point in the verticle profile of the spiral. Faller (1965, 1966) found that because of this inflection

point, eddies in a turbulent Ekman layer will take the form of horizontal rolls aligned along the direction of the mean wind. The predicted dimensions of these rolls agree well with observations.

LeMone (1973) presents a roll energy budget equation in which she demonstrates that roll production energy can come from three sources: buoyancy, vertical wind shear along the roll axis (which she calls parallel instability) and shear in the cross-wind profile (the Ekman spiral shear, which she calls "inflectional instability"). Kuettner's model is a combination of buoyancy and parallel instability; Faller uses inflectional instability.

LeMone also provides us with a PBL Reynolds number, which compares the magnitude of the above two models. The number is

$$Re = \frac{2\,V_g}{f\,d}, \qquad (1)$$

where $\underline{V_g}$ is the geostrophic wind and $\underline{d}$ is the Ekman layer depth defined as

$$d = \left(\frac{2\,K}{f}\right)^{1/2} . \qquad (2)$$

Here $\underline{K}$ is the kinematic viscosity coefficient and depends on the height of the PBL.

For values of Re less than about 300, parallel instability should be the dominant mode of roll production. For Re larger than 300, "inflectional instability" is more important. LeMone's observations indicated that the latter mechanism was more appropriate: the roll

structure that it predicted resembled her data very well. The values of Re calculated by LeMone ranged from 2100 to a low of 500. No Re below 500 were observed.

LeMone's rolls occurred over the Great Plains or the Great Lakes and were associated with moderately strong daytime surface winds forced by the geostrophic wind aloft. However, the rolls seen from the April cruise data were created over the ocean at night and were associated with a region of buoyant uplift: the nearshore land breeze convergence zone. For this reason, we should expect the rolls to be a product of buoyancy and vertical wind shear parallel to the roll axis, much like the rolls inferred by Woodcock. In our case the strong vertical shear is a consequence of the low velocity land breeze undercutting the strong, southward coastal wind; we can expect the negative v-component of wind velocity to increase sharply with height. If it is true that the rolls here are produced by the parallel instability mechanism, we should get a low Re.

Before we can solve (1) and (2), we must know $\underline{K}$, which in turn is related to the height $\underline{H}$ of the PBL. We can estimate $\underline{H}$ from the dimensions of the rolls themselves. Both Kuettner and LeMone found that $H \approx L/3$, where $\underline{L}$ is the horizontal roll wavelength. For our case we get

$$L = 4.66 \text{ km} \longrightarrow H = 1.55 \text{ km}. \qquad (3)$$

From Berry, et al. (1945)

$$K = (\text{constant})\ H^2$$

$$K = (5.8 \times 10^{-6}\ \text{sec}^{-1})\ (1550\ \text{m})^2$$

$$\underline{\underline{K = 13.99\ \text{m}^2\ \text{sec}^{-1}}} \qquad (4)$$

Now we can solve for d:

$$d = \left(\frac{2\ K}{f}\right)^{1/2} \qquad (2)$$

For Oregon, f 10^{-4} sec^{-1}, so

$$\underline{\underline{d = 529\ \text{m.}}} \qquad (5)$$

Finally, if we estimate V_g to be 10 m/sec, which is approximately the value of the coastal wind observed during the cruise, we get for Re

$$Re = \frac{2\ V_g}{f\ d} \qquad (1)$$

$$Re = \frac{(2)\ (10\ \text{m sec}^{-1})}{(10^{-4}\ \text{sec}^{-1})(529\ \text{m})}$$

$$\underline{\underline{Re = 378 \pm 80\ .}} \qquad (6)$$

To get the $\pm$ 80 uncertainty in (6), we assume a $\pm$ 10% uncertainty in both the geostrophic wind V_g and the roll wavelength L. Even with this uncertainty we get a value for Re lower than those observed by LeMone, indicating that over the ocean, at least, or during this particular land breeze situation, buoyancy and parallel instability play a more significant part in the production of rolls than they do over land.

In conclusion of this section on horizontal roll vortices, Figure 21 is presented as a hypothetical situation in which all the features noted in this section are combined. The time is after midnight. The land breeze convergence zone has established itself over triangles B and C. Air is flowing seaward down the density gradient at 2 m/sec. As the dense air advances, the warmer marine air experiences buoyant uplift and rises at the main convergence zone. However, there is a strong vertical shear in effect along a line parallel to the coast, due to the southward blowing coastal wind of 10 m/sec. being displaced by the low velocity land air mass. Because of the shear, rising air has a higher relative vorticity than the surrounding air. The high vorticity air returns to its original level by describing a helical circulation seaward of the convergence zone. This produces a region of downdraft, of diverging surface winds. Low vorticity air brought down by the divergence regains its level by forming another convergence zone and rising, and so on. Thus, the competition between the buoyancy at the main convergence zone and the vorticity restoring forces due to the parallel vertical wind shear combine to induce a series of roll vortices that propagate seaward and redistribute the vorticity. The rolls migrate over triangle A, causing 37 minute periodicities in the divergence record and in the u-component of wind velocity at S5 and S3. The correlation between u and divergence is positive at S3 and negative at S5 due to the geometry of the

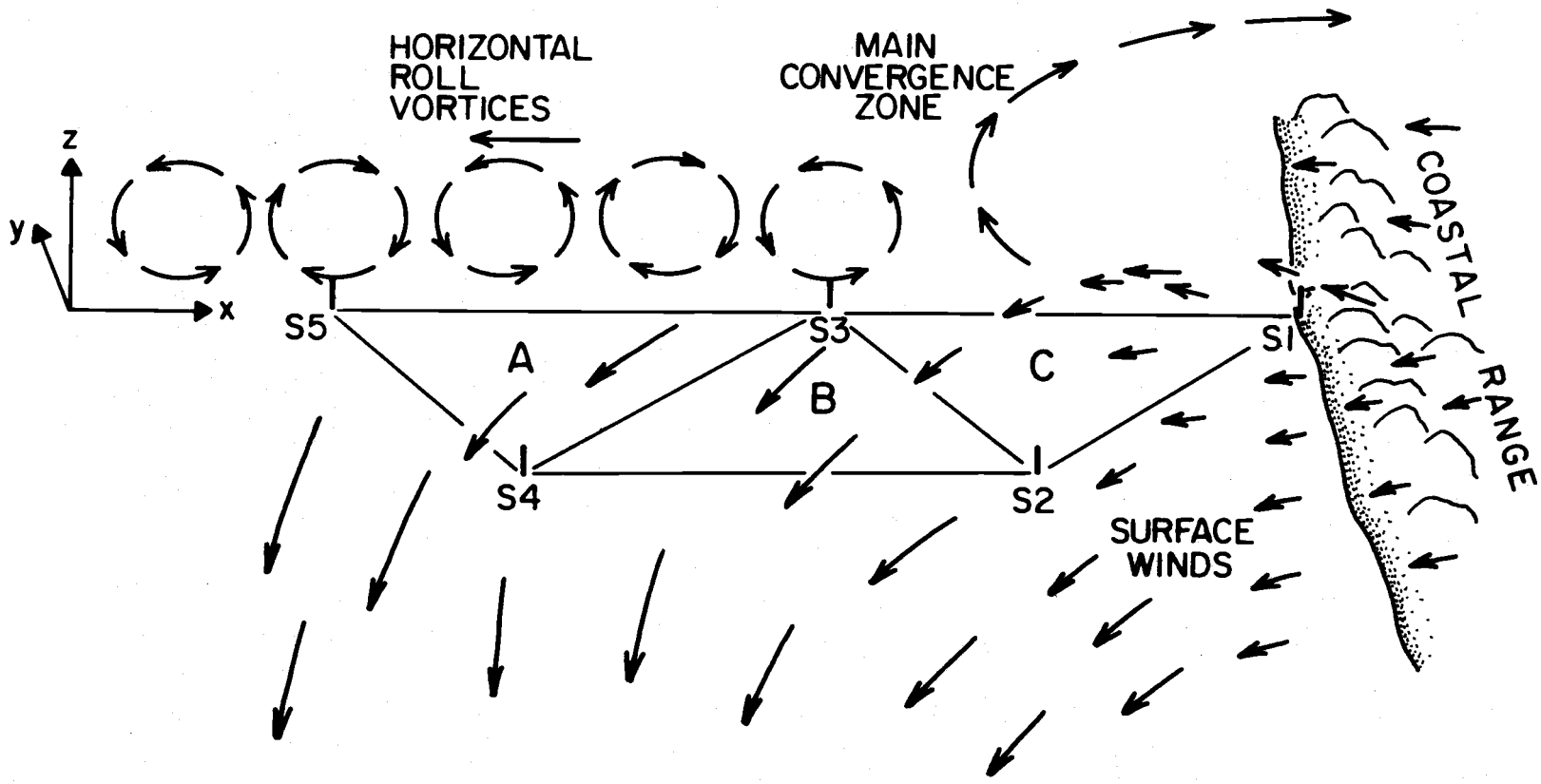

Figure 21. Hypothetical Situation at 0200.

array. The width of an individual vortex is 2.33 km, the roll wavelength is 4.66 km, and the height of the PBL is 1.55 km. The offshore migration speed is 2 m/sec. This situation exists for less than five hours, then the thermal gradients weaken, the main convergence zone fades out and the unreplenished rolls migrate away from the array and out to sea.

V. CONCLUSIONS

One of the major findings of the cruise is that significant land breezes do occur off Oregon, despite the cold water temperatures. It is not known how dependent the land breezes are on the current synoptic situation or the time of year; future experiments must first reexamine coastal wind and temperature data to determine the predictability of the events. The land breeze appeared following a cooling-off period after sunset. Instead of the strong wind of the the sea breeze, the land breeze caused a decrease in wind speed, accompanied by a temperature drop; the effect was less intense farther offshore. The fact that the wind speed decreased may be due to the existence of a fairly strong coastal wind before the events; as the coastal wind was displaced by the advancing land breeze front, the surface winds were replaced by the low velocity land air mass. Experiments must be conducted during various coastal wind situations to explain the observed decrease in wind speed. Wind velocity veered during the events, changing from a strong southward wind to a weak westward one.

Perhaps the mixing with the southward flowing marine air produced the spans of positive vorticity that covered each event, although it is possible that they were due to some other movement related mechanism. The land breeze also produced a noticeable convergence

zone in the nearshore region, that was preceeded by a divergence peak. This was probably the main zone of buoyant uplift of the warmer marine air by the denser land air. No convergence zone appeared offshore, instead there came the interesting fluctuations in divergence and u-component.

Analysis of the fluctuations revealed a 37 minute period and strong positive and negative correlation between the divergence and the u-component of wind velocity at S3 and S5. The observed periodicity and correlation fit neatly into a model of horizontal roll vortices aligned along the mean wind direction and migrating seaward. The conditions for roll production seem to favor the buoyancy and parallel instability mechanisms, instead of the inflectional instability mechanism. It seems plausible that the nearshore convergence zone is responsible for the initial upward displacement of air that eventually resulted in rolls.

The size of the observed rolls was inferred from the dimensions of the sensor array and was in agreement with previous observations. A variable spacing array, for example, the use of free floating spar buoys that could be relocated at various intervals, would be more suitable for determining the time and length scales of the rolls.

This study does not show how homogeneous the land breeze is along the coast or how far its effect reaches offshore; future buoy arrays must be established both parallel and perpendicular to the

coast. The vertical structure of the land breeze could be investigated with pibal and rawinsonde soundings. The soundings could be made both onshore and at sea, the latter by using the sextant-pelorus method described by Quinn, et al., 1970.

A tethersonde could be used to study both the land breeze and roll vortices. It could be towed behind a ship at various altitudes to obtain vertical temperature and humidity structure. Towing the tethersonde in a cross-wind direction would cause the kite to pass through a number of roll vortices' convergence and divergence bands. The response of the kite to the alternating rising and sinking air would appear as fluctuations in the pressure record from the sonde.

Similar measurements could be made with an airplane or a glider. A crop duster could release powder or smoke to delineate helical air circulations in the rolls (Crew, 1974). A sailplane is extremely responsive to regions of updraft and could track the advance of rolls by soaring over a migrating convergence zone.

Further study of the land breeze may be beneficial in many ways. The land breeze probably helps to flush polluted air out of coastal cities (Crew, 1974). It would be useful to air pollution control to be able to predict this effect. The interaction of the seaward breeze and prevailing winds may affect coastal weather, ocean surface currents and upwelling. These factors are important to many fishing operations.

Finally, since horizontal roll vortices have been associated with mixing in the PBL, it is necessary to understand how the land breeze produces and maintains roll vortices. This thesis concludes that a better understanding of the land breeze is essential for more insight into the complicated interactions of air, land and sea.

BIBLIOGRAPHY

Angell, J. K., D. H. Pack, and C. R. Dixon. 1968. "A Lagrangian Study of Helical Circulations in the Planetary Boundary Layer," Journal of the Atmospheric Sciences, 25, pp. 707-717.

Berry, F. A., E. Bollay, and N. Beers. 1945. Handbook of Meteorology, McGraw-Hill Book Co., 1068 p.

Bourke, R. H., B. Glenne, and B. W. Adams. 1971. The Nearshore Physical Oceanographic Environment of the Pacific Northwest Coast, Ref. 71-45, Department of Oceanography, Oregon State University, pp. 31-71.

Crew, H. 1974. Personal communication.

Cummings, T. K. 1973. "The Mesoscale Wind Field During Project JASIN 1972," M. S. Thesis, Oregon State University, 56 p.

Eddy, A. 1966. "The Texas Coast Sea Breeze: A Pilot Study," Weather, 21(5), pp. 162-170.

Estoque, M. A. 1961. "A Theoretical Investigation of the Sea Breeze," Quarterly Journal of the Royal Meteorological Society, 87(372), pp. 136-146.

_____ 1962. "The Sea Breeze as a Function of the Prevailing Synoptic Situation," Journal of the Atmospheric Sciences, 19(3), pp. 244-250.

Faller, A. J. 1965. "Large Eddies in the Atmospheric Boundary Layer and Their Possible Role in the Formation of Cloud Rows," Journal of the Atmospheric Sciences, 22, pp. 176-184.

Faller, A. J. and R. E. Kaylor. 1966. "A Numerical Study of the Instability of the Laminar Ekman Boundary Layer," Journal of the Atmospheric Sciences, 23, pp. 466-480.

Fisher, E. L. 1960. "An Observational Study of the Sea Breeze," Journal of Meteorology, 17(6), pp. 645-660.

Graham, R. D. 1953. "A New Method of Computing Vorticity and Divergence," Bulletin American Meteorological Society, 34(2), pp. 68-74.

Haurwitz, B. 1947. "Comments on the Sea Breeze Circulation," Journal of Meteorology, 4(1), pp. 1-8.

Haltiner, G. J. and F. L. Martin. 1957. Dynamical and Physical Meteorology, McGraw-Hill Book Co., 470 p.

Hsu, S. A. 1970. "Coastal Air-Circulation System: Observations and Empirical Model," Monthly Weather Review, 98(7), pp. 487-509.

Kuettner, J. P. 1971. "Cloud Bands in the Earth's Atmosphere: Observations and Theory," Tellus, 23, pp. 404-425.

LeMone, M. A. 1973. "The Structure and Dynamics of Horizontal Roll Vortices in the Planetary Boundary Layer," Journal of the Atmospheric Sciences, 30(6), pp. 1077-1091.

Mahrt, L. 1974. Personal communication.

O'Brien, J. J. and A. Johnson. 1973. "A Study of an Oregon Sea Breeze Event," Journal of Applied Meteorology, 12(8), pp. 1267-1283.

Ochs, L. J., J. Baughman, and J. Ballance. 1971. OS-3 ARAND System: Documentation and Examples, Vol. II, Oregon State University Computer Center, CCR-71-01, 237 p.

Panofsky, H. A. 1946. "Methods of Computing Verticle Motion in the Atmosphere," Journal of Meteorology, 3(2), pp. 45-49.

Pettersen, S. 1956. Weather Analysis and Forecasting, Vol. I, Motion and Motion Systems, McGraw-Hill Book Co., 428 p.

Quinn, W. H., D. A. Panshin, and W. V. Burt. 1970. "Method for Measuring Upper-Level Winds at Sea from Small Ships," Limnology and Oceanography, 15(5), pp. 836-838.

Schaefer, J. T. 1973. "On the Computation of the Surface Divergence Field," Journal of Applied Meteorology, 12(3), pp. 546-547.

Scorer, R. S. 1958. Natural Aerodynamics, Pergamon Press, 312 p.

Tennekes, H. 1974. "The Atmospheric Boundary Layer," Physics Today, Jan. 1974, pp. 52-63.

Wallington, C. E. 1959. "The Structure of the Sea Breeze Front Revealed by Gliding Flights," Weather, 14, pp. 263-270.

_____ 1965. "Gliding through a Sea Breeze Front," Weather, 20, pp. 140-144.

Woodcock, A. 1942. "Soaring over the Open Sea," The Scientific Monthly, 55, pp. 226-232.

APPENDIX

APPENDIX: Program DIVORT

```
C******A PROGRAM FOR THE COMPUTATION OF HORIZONTAL
C******DIVERGENCE AND VERTICAL
C******VORTICITY OVER A POLYGONAL ARRAY.  THE INPUTS
C******ARE
C******THE NUMBER AND LENGTHS OF THE FACES OF THE
C******POLYGON, ITS AREA,
C******THE DIRECTION OF THE OUTWARD NORMAL VECTOR OF
C******EACH FACE RELATIVE TO TRUE NORTH AND THE WIND
C******VELOCITY DATA.
      DIMENSION ITIME(4),DIR(99),WS(99),VDIR(99,2),FL(99)
      DIMENSION FORM1(10),FORM2(10),DON(99),VN(99,2),VT
     1(99,2)
      DIMENSION VD(99),VV(99)
      KK=INCHAR(FORM1,4HINPU,4HT FO,4HRMAT,4H IS,
     14H....)
      KK=INCHAR(FORM2,4HOUTP,4HUT F,4HORMA,4HT IS,
     14H....)
      NFACES=DECIN(4NUMB,4HER O,4HF FA,4HCES=)
      NLINES=DECIN(4HLINE,4HS OF,4H DAT,4HA= )
      AREA=DECIN(4HAREA,4H OF , 4HPOLY,4HGON ,4H(MET,
     14HERS*,4H*2)=)
      DO 10 I=1,NFACES
      WRITE(61,4)I
 4    FORMAT(' LENGTH OF SIDE',I2,' IN METERS')
      FL(I)=DECIN(4H....)
      WRITE(61,6)I
 6    FORMAT(' ANGLE FORM NORTH OF SIDE ',I2,' OUTWARD
     1NORMAL')
      DON(I)=DECIN(4H....)
10    CONTINUE
      KOUNT=0
      DO 100 I=1,NLINES
      READ(1,FORM1)(ITIME(L),L=1,4),((WS(K),DIR(K)),K=1,
     1NFACES)
      DO 90 J=1,NFACES
      DO 89 K=1,2
      L=J
      II=K. EQ. 2
      JJ=J. EQ. NFACES
      IF(II) L=J+1
      OF(II. AND. JJ) L=1
```

```
      VDIR(J,K)=DON(J)-DIR(L)
      IF(VDIR(J,K). GE. 180.) GO TO 20
      IF(VDIR(J,K). LE. -180) GO TO 30
      GO TO 40
 20   VDIR(J,K)=360. -VDIR(J,K)
      VDIR(J,K)=-1.*VDIR(J,K)
      GO TO 40
 30   VDIR(J,K)=-1.*VDIR(J,K)
      VDIR(J,K)=360. -VDIR(J,K)
 40   VDIR(J,K)=.017453*VDIR(J,K)
      VN(J,K)=WS(L)*COS(VDIR(J,K)
      VT(J,K)=WS(L)*SIN(VDIR(J,K))
 89   CONTINUE
      VD(J)=(VN(J,1)+VN(J,2))/2.
      VV(J)=(VT(J,1)+VT(J,2))/2.
 90   CONTINUE
      SUMD=0.
      SUMV=0.
      DO 99 J=1,NFACES
      SUMD=SUMD+VD(J)*FL(J)
      SUMV=SUMV+VV(J)*FL(J)
 99   CONTINUE
      DIV=SUMD/AREA
      VORT=SUMV/AREA
      KOUNT=KOUNT+1
      WRITE(2,FORM2)(ITIME(L), L=1,4), DIV, VORT, KOUNT
100   CONTINUE
      ENDFILE 2
      END
```